



Fuel Cell Systems: Total Cost of Ownership

Max Wei¹, Ahmad Mayyas², Timothy E. Lipman³, Hanna Breunig¹, Roberto Scataglini¹, Shuk Han Chan⁴, Joshua Chien⁴, David Gosselin⁴ and Nadir Saggiorato¹

¹Sustainable Energy Systems Group, Energy Analysis and Environmental Impacts Department, Environmental Energy Technologies Division, Lawrence Berkeley National Laboratory, Berkeley, CA, USA

²Department of Civil Engineering, Transportation Sustainability Research Center, University of California, Berkeley, CA, USA

³Transportation Sustainability Research Center, University of California Berkeley, Berkeley, CA, USA

⁴Department of Mechanical Engineering, University of California, Berkeley, CA, USA

Article Outline

Glossary

Definition of the Subject

Introduction

Modeling Approach

Fuel Cell System Designs and Functional Specifications

Total Cost of Ownership Modeling Results

Summary

Future Directions

Bibliography

Glossary

Fuel cell an electrochemical technology that can produce electricity or heat from a cell or a repeating unit that converts chemical energy from a fuel into electricity.

PEM fuel cell a type of fuel cell which operates at low temperature (50–100 °C) and has a

polymer electrolyte membrane between the cell anode and cathode.

SOFC fuel cell a type of fuel cell (solid oxide fuel cell) that operates at higher temperatures (500–1000 °C) and which has a solid oxide or ceramic electrolyte.

MEA (membrane electrode assembly) and EEA (electrode electrolyte assembly) the electrochemical unit cell for PEM and SOFC, respectively, with anode/electrolyte/cathode layer composition specific to each technology.

Fuel cell stack a collection of unit fuel cells connected in series form a fuel cell stack.

Fuel cell system a fuel cell stack and associated balance of plant components that together make up an entire system.

Balance of plant the balance of system components that are needed to form a complete fuel cell system such as electronic components, pumps and compressors, meters and sensors, heat exchange equipment, enclosures, etc. but not including the fuel cell stack itself.

CHP (combined heat and power) a form of distributed generation (e.g., internal combustion engine or fuel cell system) that produces both electricity and heating energy at a local site, e.g., at a building or industrial site.

Criteria air pollutants six common air pollutants found all over the USA (ground level ozone, carbon monoxide, sulfur dioxide, particulate matter, lead, and nitrogen dioxide). These pollutants can be harmful to human health and the environment and cause property damage. Fuel combustion can be one source of criteria air pollutants.

Externalities in this context externalities refer to criteria pollutants and CO₂ that are produced by a power generation source and whose net health and environmental effects may not be reflected in the cost of that generation source.

Life-cycle cost (LCC) model an LCC model for a fuel cell system includes capital and installation costs, fuel and operations, stack replacements, and end-of-life costs.

Life-cycle impact assessment (LCIA) model an LCIA model provides an estimation

of monetized health and greenhouse gas (GHG) costs from avoided emissions of CO₂ and criteria pollutants during fuel cell system operation, in addition to conventional life-cycle costs.

Total cost of ownership the total costs of owning and operating an energy system such as fuel cell CHP system including capital and installation costs, fuel costs, operating and maintenance costs, and ancillary financial costs and benefits such as carbon credits, avoided heating or cooling equipment, valuation of externalities, and any end-of-life equipment or material recovery costs.

FCS Fuel cell system.

Definition of the Subject

Fuel cells are an electrochemical technology that are reaching the market in transportation and are a growing market in stationary power systems for backup power, primary power, combined heat and power, and materials handling equipment.

The first part of this entry describes the manufacturing cost reductions from PEM and SOFC technologies that are estimated from higher-volume fuel cell manufacturing from economies of scale and improvements in overall yield.

Fuel cells combined heat and power systems have the capability to displace grid electricity and on-site fuel combustion. In general CHP systems can be used in industrial and commercial building applications. This work focuses on FC CHP in commercial building applications.

Depending on the building application and location, the FCS can result in lower CO₂ and criteria emissions, and this can lead to better societal outcomes in human health and the environment.

This second part of this entry describes the treatment of total cost of ownership for fuel cell systems illustrating the valuation of these externality benefits in different cities in the USA and how they can reduce the TCO of these systems.

This entry highlights the importance of including externalities in overall societal cost calculations in cleaner forms of energy supply systems and should be included in policy discussions for fuel cell systems that comprehend overall both public and private costs and benefits.

Introduction

As the world moves toward a more carbon-constrained economy, a better understanding of the costs and benefits of “cleaner” technology options such as fuel cells is critically needed as industry and governments make research, development, and deployment funding decisions and as organizations and individuals make long-term investment decisions. In addition to automotive applications, fuel cell systems are also being considered for a range of stationary and specialty transport applications due to their ability to provide reliable power with clean direct emissions. Existing and emerging applications include primary and backup power, combined heat and power [1], auxiliary power applications in shipping and trucking, and material handling applications such as forklifts and pallet trucks.

As an electrochemical energy-conversion process, fuel cells have intrinsically higher efficiency and much lower criteria pollutant emissions than coal or gas combustion-based plants. Current fuel cell applications range between automotive, residential, and commercial applications. Unlike automotive applications, stationary applications of the fuel cells are also less constrained to the weight and size limitations of vehicles. Fuel cells can serve as a reliable source of baseload power in comparison to variable wind or solar photovoltaic supply sources. If fuel cells become more widely deployed, they could improve public health outcomes due to the reduction air pollutants such as SO_x and fine particulate matter from traditional coal-based power plants. Fuel cell systems can also be used as distributed generation systems with supplying power close to load, where they avoid transmission line construction or line losses. Natural gas supplied fuel cell systems result in lower overall CO₂ emissions than the average US grid emissions.

Fuel cells offer a promising role in addressing energy security and carbon emissions due to their efficient energy conversion processes and clean emission profiles in comparison with fossil fuel combustion-based systems [2, 3]. In particular, CHP fuel cell systems are potentially attractive applications from both an economic and

environment standpoint due to their ability to produce both power and useful heat on-site, thus augmenting any additional heat needed to meet heating demands [4]. Low-temperature polymer electrolyte membrane (PEM) fuel cells and solid oxide fuel cells (SOFC) are the primary fuel cell technologies considered here. Solid oxide fuel cells (SOFC) are ceramic-based electrolyte fuel cells that operate between 600 °C and 1000 °C. They are of particular interest in the CHP applications due to their high fuel-to-power conversion efficiency and the high quality waste heat produced [5].

Despite the numerous advantages over conventional and alternative power generation sources, fuel cells are not yet manufactured in high volumes. One main adoption barrier is the high capital costs of fuel cells [6]. Over the last decade, the Department of Energy (DOE) has supported several cost analysis studies for fuel cell systems for both automotive [7–9] and nonautomotive systems [10–13]. Most all of these studies primarily focus on the manufacturing costs associated with fuel cell system production.

This entry expands the scope and modeling capability from existing direct manufacturing cost modeling in order to quantify more fully the broader economic benefits of fuel cell CHP systems by taking into account life-cycle assessment, air pollutant impacts, and policy incentives. TCO modeling becomes important in a carbon-constrained economy and in a context where health and environmental impacts are increasingly valued.

From the perspective of the CHP system operator and owner, direct or private costs are associated with equipment costs, operations and maintenance and fuel costs, end-of-life recycling, and potential reduced costs for building operation. The key point here is that private (or direct costs) alone are not the full picture and that including both private costs and public or societal costs (e.g., health and environmental externalities and carbon credits) using a total cost of ownership framework provides a more complete assessment of overall costs and benefits. This entry in turn can be valuable input for a more comprehensive formulation of environmentally friendly technology deployment programs and policies (e.g.,

standards, incentives, education and training programs, etc.).

This entry addresses some key barriers to greater deployment of stationary fuel cell systems (FCS): high capital and installation costs with a failure to address reductions in externalized costs and the fact that potential policy and incentive programs may not value fuel cell (FC) total benefits. The model considers fuel cell systems ranging from 10 to 250 kW_e of net electrical power for PEM and SOFC combined heat and power (CHP) systems and various annual production rates (100 to 50,000 systems per year) to estimate the direct manufacturing costs for key fuel cell stack components. Sensitivity analysis is then performed to gain insight into the impacts of manufacturing parameters on fuel cell stack costs.

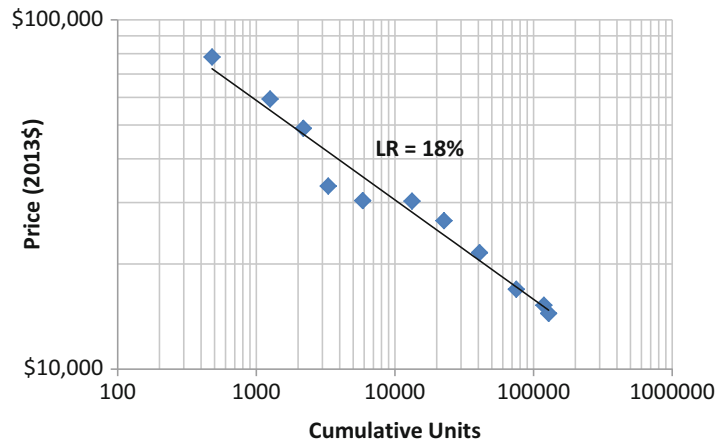
Fuel Cell Markets

Globally, fuel cell shipments have grown at 15% by MW and 37% by unit per year from 2009 to 2014, led by the stationary sector which shipped over 80% of the units in 2014 [14]. About two-thirds of MW shipped in 2014 was in Asia, led by Japan, with about 30% of total MW shipped to North America. Solid oxide fuel cell (SOFC) MW shipments have increased from 1.1 MW in 2009 to 32.3 MW in 2014 with molten-carbonate fuel cells (MCFC) growing from 18 to 70 MW. Currently, the transportation market is a very small fraction of the overall fuel cell market, but that may shift if fuel cell vehicles continue to be introduced and are more widely adopted. Toyota introduced a fuel cell passenger vehicle in November 2014 and Honda in March 2016.

Conceptually, fuel cell markets can be thought of as global markets. For example, fuel cell stack produced for vehicles should be available for the vehicles in a global market. Still, there are fuel cell systems which are geared toward specific more local markets. For example, Japan has shipped more than 100,000 micro-CHP units domestically since 2005 with an impressive overall learning rate of 18% from 2005 to 2015 (Fig. 1, where the learning rate is the empirical cost reduction in system price for every doubling of overall production volume) [15].

Fuel Cell Systems: Total Cost of Ownership,

Fig. 1 Observed cost reduction for Japan micro-CHP system cost from 2005 to 2015 with a learning rate of 18% [15]



Modeling Approach

Modeling the “total cost of ownership” (TCO) of fuel cell systems involves considering capital costs, fuel costs, operating costs, maintenance costs, “end-of-life” valuation of recoverable components and/or materials, valuation of externalities, and comparisons with a baseline or other comparison scenarios. When externalities are included in TCO analysis, both “private” and “total social” costs can be considered to examine the extent to which they diverge and there are unpriced impacts of project implementation. These divergences can create market imperfections that lead to suboptimal social outcomes but in ways that are potentially correctible with appropriate public policies (e.g., applying prices to air and water discharges that create pollution).

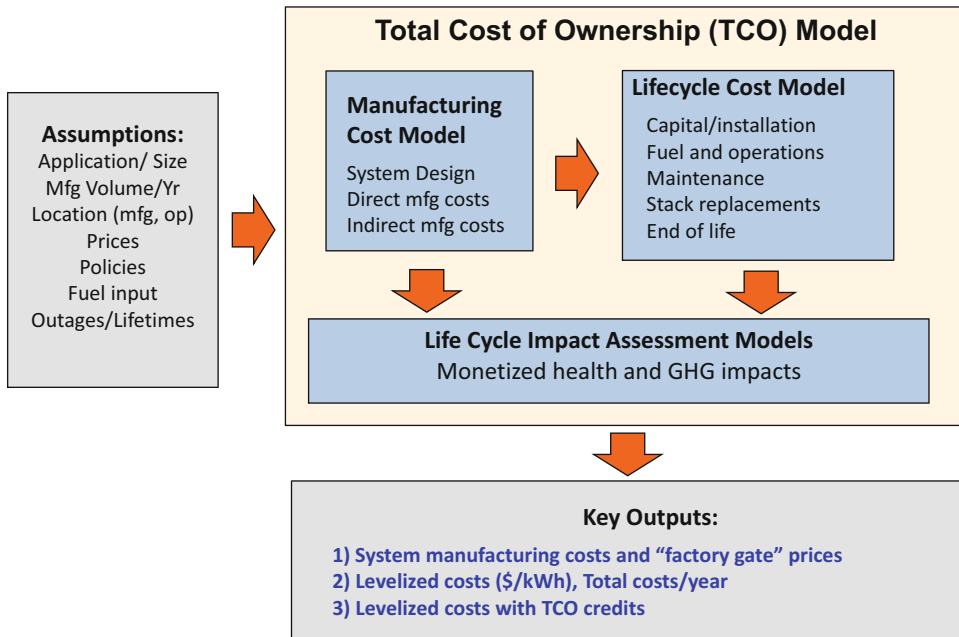
In this section the total cost of ownership modeling framework as shown in Fig. 2 is briefly described. More details on each component of the TCO model are presented in subsequent sections of this entry. The TCO model accepts assumptions about the application/size of the fuel cell system, annual manufacturing volume and year, the location of operation, prices, policies, fuel inputs, etc. The TCO model itself consists of three key components:

1. A direct manufacturing cost model for direct and indirect manufacturing costs (e.g., administrative costs)
2. A life-cycle cost (LCC) model which includes capital and installation costs, fuel and operations, stack replacements, and end-of-life costs
3. A life-cycle impact assessment (LCIA) model that provides an estimation of monetized health and greenhouse gas (GHG) costs from avoided emissions of CO₂ and criteria pollutants

Key outputs of the model include system manufacturing costs, levelized costs of power and total direct costs per year for operation, and TCO costs including broader social costs. Note however that the intent and scope of this entry is not an optimization of the fuel cell design or CHP sizing for a given commercial application but rather an illustration of the valuation of externalities.

Direct Cost Modeling Approach for Stack

This section describes the direct manufacturing cost model, which provides bottom-up costing of fuel cell stack components. Some key aspects of this modeling are shown in Fig. 3. The first step is to define the fuel cell configuration and functional specifications. Next, literature reviews and industry inputs are used to obtain functional and operational stack and system parameters referred to here as functional specifications. The system configuration and functional specifications define the system type, system size, key subsystems and system components, FC stack features, and stack and system performance specifications. These



Fuel Cell Systems: Total Cost of Ownership, Fig. 2 Total cost of ownership modeling framework

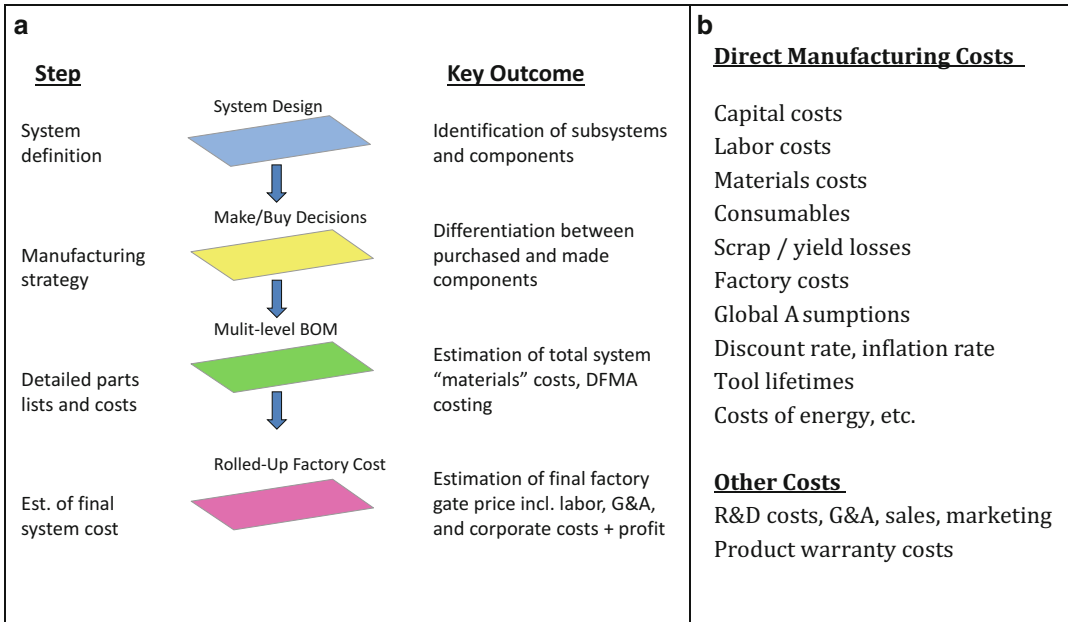
form the basis for direct manufacturing cost modeling which includes capital costs, labor costs, materials costs and consumables, scrap/yield losses, and factory building costs subject to global assumptions such as discount rate, inflation rate, and tool lifetimes. Note that process modeling or optimization of the stack design from a detailed thermodynamic and thermo-chemical point of view is not the focus of this entry. Rather, a “medium fidelity” design, based on feedback from industry advisors, is used to be representative of actual fuel cell systems.

The bottom-up or design for manufacturing and assembly (DFMA is a registered trademark of Boothroyd Dewhurst, Inc. and is the combination of the design of manufacturing processes and design of assembly processes for ease of manufacturing and assembly and cost reduction. It also refers to bottom-up cost modeling, and it is that usage that is used here.) analysis includes the following items shown in Fig. 3b for direct manufacturing costs, global cost assumptions, and other non-product costs. For each manufactured component, first a patent and literature search was done and industry advisor input elicited, followed by selection of a base

manufacturing process flow based on these inputs, an assessment of current industry tooling and direction, and engineering judgment as to which process flows can support high-volume manufacturing in the future.

Balance of plant or nonfuel cell stack components such as compressors, tubing, and power electronics is largely assumed to be purchased components, and stack components are largely manufactured in-house, with carbon fiber paper and Nafion[®] membrane, the key exceptions for reasons as described below. Vertical integration is assumed for stack manufacturing, i.e., a fuel cell manufacturer is assumed to manufacture all stack components as described below. This assumption is geared toward the case of high-volume production. At lower production volume, some purchase of finished or partially finished stack components may be cost beneficial because at very low volumes, the investment costs for vertical integration are prohibitive and equipment utilization is inefficient.

Overall manufacturing costs are then quoted as the sum of all module or component costs normalized to the overall production



Fuel Cell Systems: Total Cost of Ownership, Fig. 3 (a) Generalized roll-up steps for total system cost; (b) scope of direct manufacturing costs for components produced in-house (Wei et al. [2])

volume in kWe. Direct manufacturing costs are quoted in cost per kWe of production and are often quoted in cost per meter squared of material for roll-to-roll goods such as GDL and catalyst-coated membrane. Global costing assumptions include discount rate, inflation rate, tool lifetimes, and costs of energy (e.g., electricity and fuel). Direct manufacturing costs are quoted as the sum of fuel cell stack component manufacturing and balance of plant components. A further corporate markup will include nonmanufacturing costs such as general and administrative, sales and marketing, research and development costs, and profit margin to determine the final "factory gate" price to the customer. The installed price to the customer will also need to take into account installation costs and any other fees (e.g., permits, inspections, insurance, service contracts, etc.). Delivery/installation costs for CHP systems are expected to be highly site and project specific. The focus of this entry is on direct manufacturing costs and does not provide a detailed analysis for corporate markups or installation costs.

Manufacturing Cost Analysis: Shared Parameters

Shared parameters for the cost analysis are summarized in this section, with manufacturing cost shared parameters summarized in Table 1. References are shown in the table and are a mixture of general industry numbers (e.g., annual operating days, inflation rate, tool lifetime) together with fuel cell-specific industry assumptions (discount rate, web width, hourly wage).

An annualized cost of tool approach is adopted from Haberl [16]. The annualized cost equation and components are as follows:

$$C_y = C_c + C_r + C_{oc} + C_p + C_{br} + C_i + C_m - C_s - C_{int} - C_{dep} \quad (1)$$

where

C_y is the total annualized cost

C_c is the capital/system cost (with interest)

C_r is the replacements or disposal cost

C_{oc} is the operating costs (e.g., electricity) excluding labor

C_p is the property tax cost

C_{br} is the building or floor space cost

Fuel Cell Systems: Total Cost of Ownership, Table 1 General manufacturing cost parameters [3]

Parameter	Symbol	Value	Units	Comments
Operating hours	t_{hs}	Varies	Hours	8 h base shift; (2–3 shifts per day)
Annual operating days	t_{dy}	240	Days	52 weeks*5 days/week, 10 vacation days, 10 holidays
Avg. inflation rate	j	0.023		US average for past 10 years ^a
Avg. mortgage rate	j_m	0.051		Trading economics ^b
Discount rate	j_d	0.10		
Energy inflation rate	j_e	0.056		US average for last 3 years ^a
Income tax	i_i	0		No net income
Property tax	i_p	0.01035		US average ^c
EOL salvage value	k_{eol}	0.02		Assume 2% of end-of-life value
Tool lifetime	T_t	15	Years	Typical value in practice
Energy tax credits	ITC	0	Dollars	
Energy cost	c_e	0.10	\$ kWh ⁻¹	Typical US value
Floor space cost	c_{fs}	1291	\$ m ⁻²	US average for factory ^d
Building depreciation	j_{br}	0.031		US Department of Commerce ^e
Building recovery	T_{br}	31	Years	US Department of Commerce ^e
Hourly labor cost	c_{labor}	30	\$ hr ⁻¹	Hourly wage per worker

^aForecast-Chart, <http://www.forecast-chart.com/forecast-inflation-rate.html>, 2015

^bTrading Economics, <http://www.tradingeconomics.com/united-states/mortgage-rate>, 2015

^cTax-rates.org, <http://www.tax-rates.org/taxtables/property-tax-by-state>, 2015

^dRSMeans, <http://learn.rsmeans.com/rsmeans/models/factory2/>, 2017

^eUS Department of Commerce, Bureau of Economic Analysis, <https://www.bea.gov/>, 2015

C_i is the tool insurance cost

C_m is the maintenance cost

C_s is the end-of-life salvage value

C_{int} is the deduction from income tax

C_{dep} is the deduction due to tool depreciation

In the current version of the model C_r , the replacements or disposal cost and C_i , the tool insurance cost, are assumed to be zero. No net income for fuel cell manufacturers is assumed, as is currently the case for PEM manufacturers and thus income tax credits such as interest tax credits do not factor into the calculations below.

Factory area is incorporated by incrementally adding factory area to each specific process module. In general, factory cost contributions are found to be very small factors, especially as production volumes exceed 1000 systems per year.

The cost analysis utilizes largely existing manufacturing equipment technologies and existing materials with key exceptions to be noted (e.g., injection molding composite material for bipolar plates). It does not assume new high-speed manufacturing processes nor major fuel cell technology advances such as much lower cost catalysts or membranes, although the

manufacturing readiness of these technologies applied to fuel cell-specific modules was not evaluated. This entry is thus a “potential cost reduction” study for future costs with existing manufacturing technologies and mostly existing materials, and DOE cost targets for 2020 are used as a benchmark comparison for the cost estimates here. This entry assumes that higher overall volumes will drive significant improvements in yield, but it is not a market adoption or market penetration study and therefore timelines will vary according to the assumptions made for market adoption. Stationary fuel cell systems may also benefit from growth in the transportation sector and higher volumes achieved for fuel cell components in that sector over the next few years may reduce the cost of components for stationary applications (e.g., GDL, membranes, metal plates, etc.).

PEM Balance of Plant Cost Analysis Approach

The general approach for balance of plant costing is a cost of component costing analysis based on the system designs shown below and using information from existing fuel cell systems, industry advisors, and various FCS specification sheets for data

sources. Balance of plant components as mentioned above is assumed to be primarily purchased components.

Methods of determining the representative components found in systems models range from inspection of existing stationary fuel cell systems, information gathered through surveys of industry members, discussions and price quotes with component vendors, and utilization of components used for common but similar functions in other applications.

Life-Cycle Cost Modeling

Life-cycle cost modeling or use-phase modeling is defined as the costs associated with the ownership and operational phase of the fuel cell system when it is functioning in the field as a CHP system. For most stationary power applications, the use-phase is the most demanding phase among LCIA phases in terms of energy and cost and has the greatest GHG impact among all phases [2]. Figure 4 shows the sequence of steps in developing the use-phase model. The current use-phase model is developed for a CHP system operating on reformat fuel produced from natural gas input fuel, with the reforming process assumed to be on-site. GHG emission analysis is based on the emissions associated with the reforming process and does not include fuel extraction and transportation.

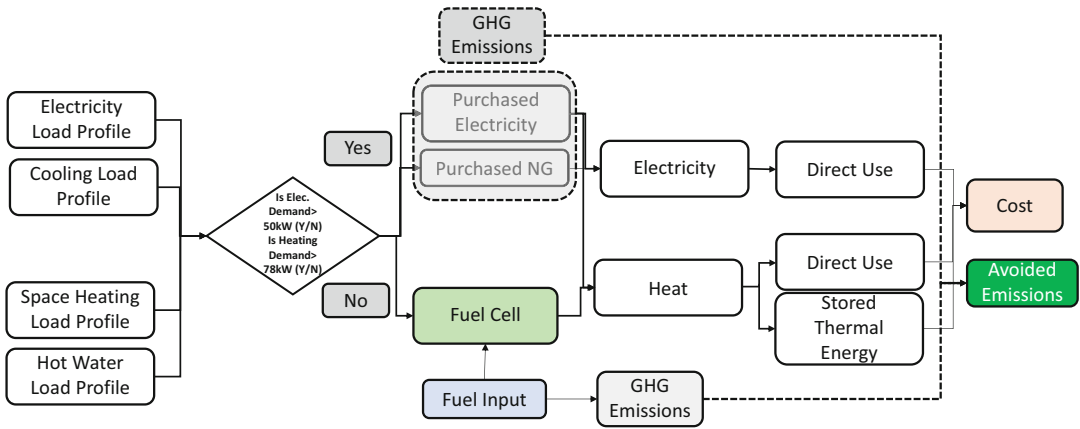
Figure 4 shows the life-cycle cost (or use-phase) modeling elements for the example of a 50 kW PEM FC combined heat and power (CHP) system. This model has four inputs: electricity demand excluding cooling loads, electricity demand for space cooling using traditional electrically driven vapor compression air conditioners, hot water heating demand, and space heating demand as a function of time, as recorded in daily load curves for 3 different days per month (weekday, weekend, and peak day). These load shapes are collected from an NREL modeling simulation [17]. The operating mode of this system will follow the total electricity load (sum of “non-cooling electricity load” and “electricity for cooling load”), so that the fuel cell system will cover all of the electrical demand at any time when total electricity demand is less than or equal to 50 kWe; however, if the total demand

exceeds fuel cell capacity (i.e., total electricity loads >50 kWe), then the system will cover the 50 kWe maximum level and the remaining will be purchased directly from the grid. Similar logic is used for heating demand. The costs of operation of the fuel cell and the purchased grid electricity and fuel for supplementary on-site heating can then be calculated in addition to the greenhouse gas (GHG) emissions associated with the fuel cell operation and those from the electricity grid and on-site combustion of any fuels.

In general, building types with relative high fraction of heat loads relative to overall on-site energy consumption are favorable to CHP systems. In this entry small hotels in five cities are used as building examples. Building load shapes are drawn from five cities representing different climate zones in the USA (New York, Chicago, Minneapolis, Houston, and Phoenix). Utility tariffs are drawn from the OpenEI database (http://en.openei.org/wiki/Utility_Rate_Database) of national utility rates and include electricity rates in \$/kWh, demand charges (\$/kWe (max) per month), and other fixed charges. Natural gas fuel prices are based on the average state commercial price of gas from 2011 to 2014 for each location, since prices are variable and a point estimate for prices may be misleading.

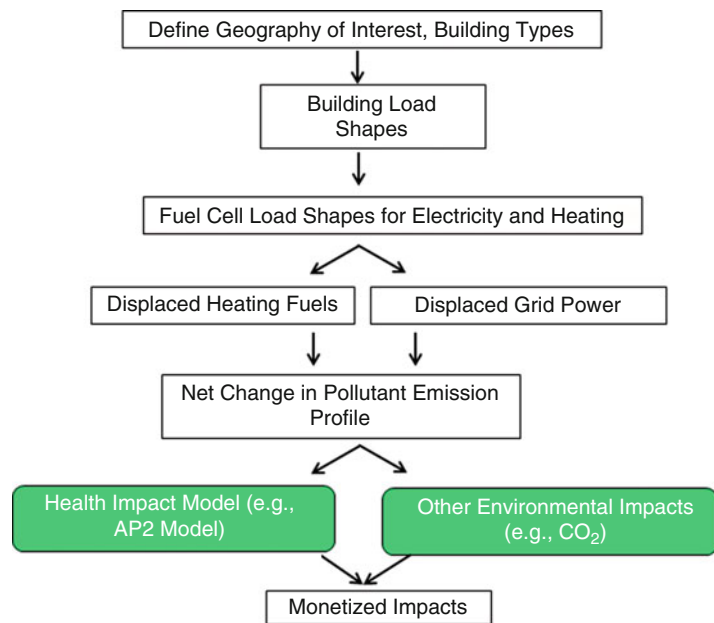
Life-Cycle Impact Assessment Modeling

Figure 5 shows the elements of the life-cycle impact assessment (LCIA) model to quantify the environmental and human health impacts and/or benefits attributable to the use of fuel cell systems in commercial buildings. The model provides spatial resolution at the state level for electricity generation impacts and at the county level for on-site fuel consumption. The motivation for the development and application of this model is the need to assess the cost of health and environmental externalities associated with fuel cells. The use of fuel cells can impose impacts that arise from the manufacturing of the cells, the extraction of raw materials for manufacturing, fuel cell operation, and the production of energy for manufacturing, transportation, and servicing of the cell [18]. The



Fuel Cell Systems: Total Cost of Ownership, Fig. 4 Fuel cell system life-cycle cost modeling for a combined heat and power fuel cell system [2]

Fuel Cell Systems: Total Cost of Ownership, Fig. 5 Life-cycle impact assessment for environmental and health externalities [2]



impact assessment characterizes the use-phase of the fuel cell system. The use of on-site fuel cells will also offset the production of electricity in the region where the cells supply power. Fuel cell-based CHP can also offset on-site criteria pollutant emissions due to the combustion of heating fuel. This offset or net change in emissions can have health benefits that will depend on the sources of electricity in a region and the impacts associated with that electricity production.

Commercial building surveys [19] are used to estimate the mix of heating fuel types by region that is displaced by the FCS. Externalities to be valued include morbidity, mortality, impaired visibility, recreational disruptions, material damages, agricultural and timber damages, and global warming.

In this approach, a fuel cell system in a given building displaces some fraction of building electricity demand that otherwise would be purchased from the grid and some fraction of heating

demand fuel, as described in the LCC modeling section above. From this, the displaced heating fuels and displaced grid power are computed, and together with the criteria emission factors of the grid, heating fuels and the FCS, the net change in pollutant emissions is derived. Valuation of health and environmental externalities for grid-based electricity and on-site fuel consumption are calculated according to the input parameters in Table 2. Total damages or externality damages for each criteria pollutant from grid electricity, on-site heating fuel from conventional heating, and the fuel cell system are then given by

$$\begin{aligned} & \text{Health and environmental externality valuation} \\ & \text{for pollutant } i \left(\frac{\$}{MWh} \right) \text{ from grid electricity} \\ & = MEF_i^* MBA_i = \frac{\text{Ton of pollutant } i^*}{MWh(el)} \frac{\$}{\text{Ton of pollutant } i} \end{aligned} \quad (2)$$

$$\begin{aligned} & \text{Health and environmental externality} \\ & \text{valuation for pollutant } i \left(\frac{\$}{MWh} \right) \\ & \text{from heating fuel} = MEF_i^* MBA_i \\ & = \frac{\text{Ton of pollutant } i^*}{MWh(\text{thermal})} \frac{\$}{\text{Ton of pollutant } i} \end{aligned} \quad (3)$$

$$\begin{aligned} & \text{Health and environmental externality valuation} \\ & \text{for pollutant } i \left(\frac{\$}{MWh} \right) \text{ from fuel cell system} \\ & = MEF_i^* MBA_i \\ & = \frac{\text{Ton of pollutant } i^*}{MWh(el)} \frac{\$}{\text{Ton of pollutant } i} \end{aligned} \quad (4)$$

where MEF is the marginal emission factor, MBA is the marginal benefit of abatement, MWh is the quantity of electricity production or thermal energy from heating fuel in units of MWh, and the assumed emission factors and spatial regime and temporal regimes are defined as in Table 2. The externality valuations above can be interpreted as the savings to society per every unit of energy avoided from each respective source (the grid, heating fuel, or the fuel cell system). Note that electricity emissions are assumed to be stack-height level, i.e., above ground level for air-mixing purposes, and that the spatial regimes varies across the four factors. Electricity MEFs are taken from eGRID subregional factors (eGRID 2015), electricity and fuel MBAs are given by the AP2 model [20], and fuel MEFs are given by the EIA and

Fuel Cell Systems: Total Cost of Ownership, Table 2 LCIA impact assessment calculations assumptions. LCIA modeling for health/environmental valuation includes both displaced electricity and displaced on-site fuel

Type	Item	Units	Assumed source of emissions	Spatial regime	Temporal regime	Reference
Electricity from grid	MEF	Tons/MWh	Stack-height level	eGRID subregions	Annual	[21]
	MBA	\$/ton	Stack-height level	State level	Annual	[20]
Fuel for conventional heating	MEF	Tons/MWh	Ground level	Site level	Annual	[22, 23], various
	MBA	\$/ton	Ground level	County level	Annual	[20]
Electricity from fuel cell system	MEF	Tons/MWh	Ground level	Site level	Annual	Various, FCS technology-dependent
	MBA	\$/ton	Ground level	County level	Annual	[20]

MEF marginal emission factor, *MBA* marginal benefit of abatement

various sources for fuel combustion equipment. The net externalities valuation (or savings) of

the FCS can then be estimated using the net change in criteria pollutants as below:

$$\begin{aligned}
 & \text{Net health and environmental externality savings for pollutant } i \text{ from } FCS \\
 & = \Delta GWh (\text{grid electricity}) * \text{Valuation of grid electricity} \\
 & + \Delta GWh (\text{heating fuel thermal energy}) * \text{Valuation of heating fuel} \\
 & - \text{Valuation from } FCS
 \end{aligned} \tag{5}$$

where ΔGWh (grid electricity) electricity and ΔGWh (heating fuel thermal energy) are the savings in grid electricity and heating fuel, respectively.

This approach provides a greater degree of spatial resolution compared to taking national averages for MBA values, and a comparison of this treatment versus the use of national averages will be addressed in future work.

Electricity and Fuel Emission Factors

In this entry, stationary fuel cells provide electricity and heat to commercial buildings in different cities in the USA. Electricity from fuel cells displaces energy and emissions from local electricity grids, comprised of conventional and renewable generators. Over long periods of time (on the order of decades), a large reduction in demand for grid electricity may lead to the retirement of conventional generators. Only short-term displacement is considered and measured using regional marginal emission factors. Marginal emission factors (MEFs) express the avoided carbon dioxide (CO₂-eq), sulfur dioxide (SO₂), and nitrogen oxides (NO_x), emissions from displaced marginal generators. It is difficult to know exactly which generators are operating at the margin, but the set of generators that will be deployed to meet electricity demand during high-demand periods (commonly called peaker plants) can be estimated using dispatch models and historical regressions. Subregional non-baseload emission factors from eGRID (2015) [21] are used for CO₂ (Fig. 6) and criteria emission factors. A second set of estimates based on historical regressions is provided for comparison [24]. Note that there is more than a factor of two between regional CO₂ non-baseload emission rates indicating the high range of

emission factors that exist on the US grid depending on region.

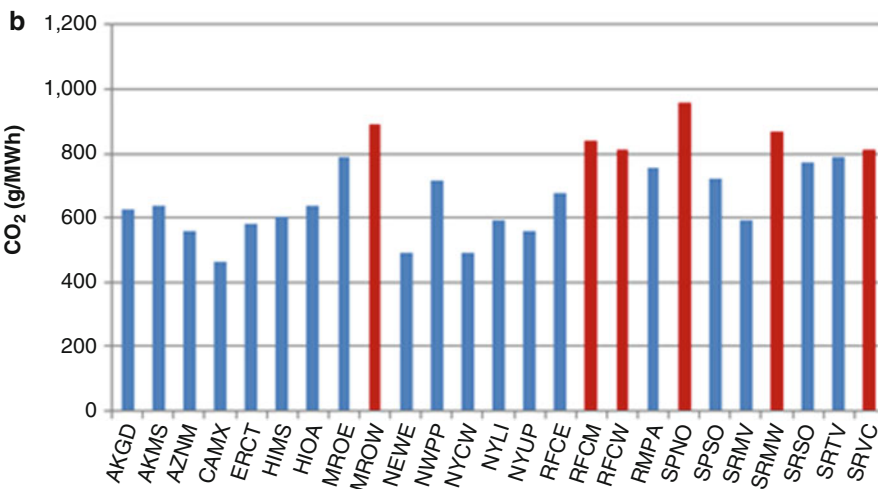
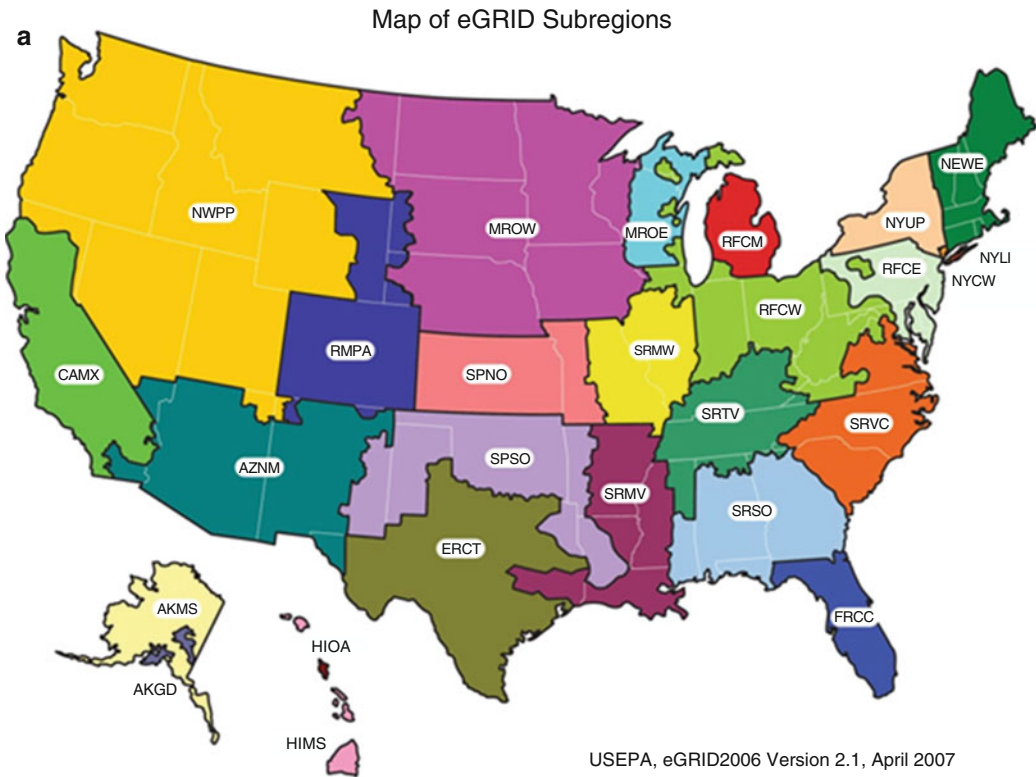
The approach here is to use MEFs for greenhouse gases (GHG) (CO₂, CH₄, and N₂O), NO_x, and SO_x. MEFs for direct particulate matter emissions (PM₁₀ and PM_{2.5}) are not included since a dominant portion of PM from electricity generation comes from reactions of SO_x and NO_x in the atmosphere. Subregional MEFs for grid-based electricity are shown in Table 3. MEFs for on-site combusted fuels are also shown [22, 23]. Commercial building surveys [19] were utilized to estimate the mix of heating fuel types by region that is displaced by the FCS.

AP2 Damage Factors

The benefit of reducing emissions through FCS adoption can be monetized using conversion factors that express marginal benefit of abatement. These factors estimate the damage that a unit of emitted pollutant will cause if released in a specific location, thus explaining their alternative name “damage factors”.

In this entry, a set of damage factors are described and applied in the Air Pollution Emission Experiments and Policy (APEEP) analysis model and its revised version (AP2). Alternatively other studies could be used for damage factors as discussed in a recent dissertation [54].

AP2 monetizes human health and environmental damages associated with SO₂, volatile organic compounds (VOC), NO_x, ammonia (NH₃), fine particulate PM_{2.5}, and coarse particulate PM₁₀ emissions from power plants (The subscript on PM indicates the greatest particle diameter in micrometers that is captured in the particle measurement.) [22] and ground level sources. The idea in APEEP and AP2 is to introduce an



Fuel Cell Systems: Total Cost of Ownership, Fig. 6 eGRID subregions and non-baseload emission rates by subregion [21]

additional metric ton of pollutant from a specific source and determine the change in national damages. This process is repeated for each pollutant type at about 10,000 sources, generating a set of

marginal damages that are more reliable than an approach based on national averages. Atmospheric chemistry models and air transport models were used to estimate downwind primary and

Fuel Cell Systems: Total Cost of Ownership, Table 3 Regional marginal emission factors for electricity and emission factors for heating fuels. All emission

factors are from eGRID [21] except for CO₂ emissions from Siler Evans [24] (note that kWh are used as heating fuel units here for natural gas, fuel oil, and propane)

	tCO ₂ /kWh	tCO ₂ /kWh [24]	tCH ₄ /kWh	tN ₂ O/kWh	tNO _x /kWh	tSO _x /kWh
Electricity (Chicago)	8.13E-04	7.31E-04			7.5E-07	2.6E-06
Electricity (Houston)	5.81E-04	5.27E-04			3.3E-07	9.23E-07
Electricity (Minneapolis)	8.92E-04	8.34E-04			1.15E-06	2.23E-06
Electricity (New York City)	4.91E-04	4.89E-04			2.87E-07	1.23E-08
Electricity (Phoenix)	5.61E-04	4.86E-04			4.69E-07	1.48E-07
Electricity (San Diego)	4.62E-04	4.86E-04			1.6E-07	1.27E-07
Natural gas	1.81E-04		1.71E-08	3.41E-10	1.51E-07	9.21E-10
Fuel oil	2.50E-04		1.02E-08	2.05E-09	3.44E-07	1.73E-06
Propane	2.10E-04		6.82E-12	3.41E-10		

secondary pollution doses. For example, SO₂ forms PM_{2.5} (sulfate), and NO is converted to NO₂, which reacts with VOC to form ozone (O₃) and PM_{2.5} (nitrate). Once the emissions and the resulting pollutants are calculated, human exposures are estimated from a database of county-level receptor populations (humans, materials, crops, timber, etc.). Damage factors were calculated for “ground level”: (less than 250 m off the ground), “medium high” (<500 m), and “tall-smoke stack” sources (>500 m). Concentration-response models are used to convert exposure to physical responses such as morbidity, mortality, visibility impairment, reduced recreation, lower agricultural and timber yields, and material degradation. Finally, economic models convert these physical responses to dollar values. In this entry, the value of a statistical life is assumed to be \$6 million and a social discount rate of 3% is assumed [20]. The implication of these values is that morbidity and mortality are valued more when they occur in younger people than in older people. The total damage from a pollutant emission from a given source is estimated by multiplying the pollutant damage factor with the mass of emitted pollutant. Given the multiple sources of uncertainty in this type of modeling, there is generally a wide range of estimates of health and environmental damages. The scope of this entry does not include a detailed uncertainty analysis of externality damages nor a comparison of outputs of AP2 and other models (see, e.g., [25]).

Marginal benefit of abatement or damage factors are shown in Tables 4 and 5 for ground level and stack-height level emissions, respectively, for the regions of the USA studied.

Emissions from Fuel Cells

Direct emission factors reported in recent literature on fuel cells allowed us to determine reasonable EF for CO₂, CH₄, N₂O, CO, NO_x, SO_x, PM₁₀, and VOC (Table 6). PEM values are based on Colella [26], and SOFC values are from NETL [27] and [1].

Fuel cell emissions are modeled as ground level emissions and were converted to damages using AP2 county ground level damage factors. CO₂, CH₄, and N₂O are converted to CO₂eq using 100-year GWP factors of 1, 21, and 310, respectively (http://www.ipcc.ch/publications_and_data/ar4/wg1/en/ch2s2-10-2.html, accessed September 25, 2009).

The total masses of emissions emitted from the fuel cell over a year are calculated by multiplying each EF by the power (P) provided by the fuel cell in our scenarios. Emissions from the fuel cell are modeled as ground level emissions and are converted to damages using AP2 county-specific ground level conversion factors shown in Table 4.

Greenhouse gas emissions were converted to CO₂eq using a 100-year global warming potential and monetized by assuming a social cost of carbon (SCC), of \$44/tCO₂eq. Values for the social cost of carbon have been compiled by the

Interagency Working Group on Social Cost of Carbon [28], for use in regulatory analysis. As a base value for additional examination, an intermediate value of \$37/tCO₂ (\$2007) is used and adjusted for inflation to get ~\$44/tCO₂ as an approximate value of the current social cost of carbon.

Emission Factor Projections with Proposed Clean Power Plan

The analysis described above provides a snapshot in time of the health and environmental impacts of a fuel cell CHP system for a given year, e.g., for eGRID emission factors for 2012, the most recent year available from the EPA. Of course, the electricity grid is not a static entity in terms of its generation portfolio and emission factors. The proposed EPA Clean Power Plan (The CPP is still being

reviewed in US Court of Appeals but is assumed to be enacted for the purposes of this study. It is unclear at the time of this writing if the CPP will be rolled back in scope or replaced with new legislation. As of April 28, 2017, “the US Court of Appeals for the District of Columbia Circuit this morning granted the White House’s request for pause in litigation on the Clean Power Plan, holding the case in abeyance for 60 days.” (<http://www.utilitydive.com/news/dc-circuit-halts-clean-power-plan-case-in-win-for-trump/441554/>, accessed May 29, 2017.) (CPP) to 2030 if enacted would result in a cleaner grid electricity than that of 2012 [29] and would reduce the health and environmental benefits from fuel cell CHP. The CPP improve emissions from existing coal plants and shift from coal to natural gas and build more renewable sources of electricity. The key objective here is to try to estimate the impact that

Fuel Cell Systems: Total Cost of Ownership, Table 4 Marginal benefit of abatement for ground level emissions in dollars per metric ton for the six counties in this study (in 2014 dollars). Statistical life value of \$6 million is assumed [20]

City	County	State	Ammonia	Nitrogen oxides	Sulfur dioxide	Volatile Organic compounds	Particulate matter	Particulate matter
			\$/ton NH ₃	\$/ton NO _x	\$/ton SO ₂	\$/ton VOC	\$/ton PM _{2.5}	\$/ton PM ₁₀
Chicago	Cook	IL	10,497	90,199	169,705	44,959	471,416	18,335
Houston	Harris	TX	11,526	5695	27,349	5151	53,952	5679
Minneapolis	Hennepin	MN	3808	70,544	122,325	30,186	316,990	13,771
New York	New York	NY	102,744	33,935	166,045	71,370	765,320	30,403
Phoenix	Maricopa	AZ	4254	23,003	39,007	10,256	109,293	3005
San Diego	San Diego	CA	16,948	62,821	330,921	32,929	350,036	13,313

Fuel Cell Systems: Total Cost of Ownership, Table 5 Marginal benefit of abatement for stack-height level emissions in dollars per ton (in 2014 dollars) for the

six states in this study (point sources with height >250 m and <500 m and statistical life value of \$6 million) [20]

State	Ammonia	Nitrogen oxides	Sulfur dioxide	Volatile organic compounds	Particulate matter	Particulate matter
	\$/ton NH ₃	\$/ton NO _x	\$/ton SO ₂	\$/ton VOC	\$/ton PM _{2.5}	\$/ton PM ₁₀
Arizona	2642	4989	11,142	1250	13,208	469
California	12,462	4005	24,704	3490	37,052	1689
Illinois	5977	9052	27,370	3531	36,767	1213
Minnesota	3090	8252	23,669	2256	23,516	853
New York	42,470	3155	23,705	5792	61,371	2024
Texas	1976	6120	10,448	1621	17,020	594

these changes to the electricity grid would have on the externality benefits of fuel cell CHP.

Table 7 shows estimated CPP impacts to grid electricity carbon intensity and criteria emission intensity. Demands from the AEO2015 base case for 2025 are extrapolated to 2030 and assume a nominal 7% demand reduction from energy efficiency to 2030 demands from the Clean Power Plan in all regions per [30]. CO₂ reductions are taken from mass-based reduction targets in the Clean Power Plan. Note that the regulations for CO₂, SO₂, and NO_x emissions are not the same. The Clean Power Plan regulates CO₂, and this impacts SO₂ and

NO_x; but SO₂ and NO_x have existing regulations with a base emission reduction in tons of 70% and 25%, respectively, in 2025 from 2012 (Mercury and Air Toxics Standards or MATS). Here, it is assumed that the same percentage reduction in MEF from the CPP as the estimated percent reduction in AEF from CPP. For regions where gas is already on the margin, this may be an overestimate, but for regions for which coal is currently on the margin, this may be an underestimate in the percentage reduction.

Fuel Cell Systems: Total Cost of Ownership, Table 6 Fuel cell emission factors in metric tons per kWh for a PEM FC CHP system with reformat and natural gas fuel input

Pollutant	Emissions in tons/kWhe PEM	Emissions in tons/kWhe SOFC
CO ₂	5.43E-04	3.4E-04
NO _x	7.5-09	Negligible
SO _x	Negligible	Negligible
PM ₁₀	Negligible	Negligible
VOC	Negligible	Negligible
CH ₄	5.6E-07	5.6E-07
CO	1.9E-08	Negligible
N ₂ O	6.5E-08	6.5E-08

Levelized Cost of Electricity with Total Cost of Ownership Credits

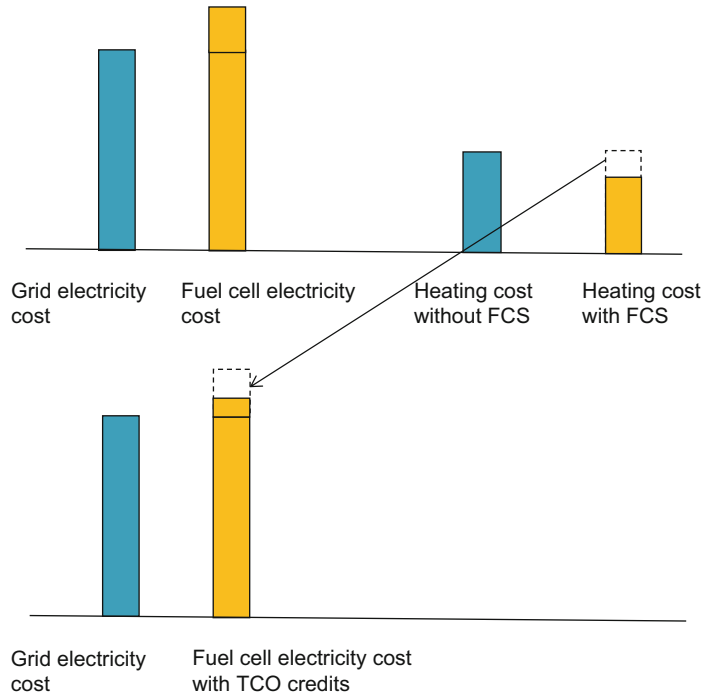
Figure 7 illustrates the conceptual approach used to compare the case of fuel cell CHP total cost of ownership with a reference case of no FCS, grid-based electricity, and conventional heating equipment. A fuel cell CHP system will typically increase the cost of electricity but provide some savings by offsetting heating energy requirements. The cost of fuel cell electricity in this case is taken to be the “levelized cost of electricity” (LCOE) or the levelized cost in \$/kWh for the fuel cell system taking into account capital costs, operations and maintenance (O&M), fuel, and capital replacement costs (inverter, stack replacement, etc.) only. In

Fuel Cell Systems: Total Cost of Ownership, Table 7 Estimated Clean Power Plan impacts for six representative regions

City	eGRID subregion	kg/MWh			kg/MWh			% Reduction 2030 from 2012		
		eGRID for 2012			2030 Projection with Clean Power Plan			CO2	SO2	NOx
		CO2 AEF eGRID	SO2 AEF eGRID	NOx AEF eGRID	CO2 AEF	SO2 AEF	NOx AEF			
Minneapolis	MROW	646	1.33	0.73	489	0.25	0.45	24%	81%	38%
NYC	NYCW	316	0.03	0.15	322	0	0.05	-2%	97%	64%
Chicago	RFCW	626	1.54	0.55	510	0.4	0.34	19%	74%	37%
Houston	ERCT	518	0.87	0.28	440	0.09	0.11	15%	90%	61%
Phoenix	AZNM	523	0.2	0.59	459	0.07	0.3	12%	64%	50%
San Diego	CAMX	295	0.09	0.15	259	0.03	0.08	12%	62%	46%
Average								13%	78%	49%

Fuel Cell Systems: Total Cost of Ownership,

Fig. 7 Cost of energy service for fuel cell CHP and conventional electricity and heating systems. A fuel cell CHP system will typically increase the levelized cost of electricity (upper left two bars). But if waste heat is utilized, the cost of heating is reduced (upper right two bars). In this treatment, all nonelectricity credits (heating fuel savings, carbon credits, societal health, and environmental benefits) are applied to an LCOE with TCO credits or a “total cost of electricity”



this entry, in addition to crediting the heating fuel savings to the $LCOE_{FC}$, carbon credits from net system savings of CO_{2eq} and net avoided environmental and health-based externalities are credited to the fuel cell system cost of electricity. The resultant quantity is the “cost of electricity with total cost of ownership credits or savings.” This allows comparison of fuel cell cost of electricity with TCO credits to the reference grid electricity cost (\$/kWh).

More specifically, this comparison is described by the equations below. For a representative commercial building (e.g., hotel, hospital, college dormitory), the “no fuel cell system” case has an overall cost of electricity as follows:

$$\text{Cost of electricity } \left(\frac{\$}{kWh} \right) = \frac{\text{Annual energy cost} + \text{Annual demand charges} + \text{Other Charges}}{\text{Total electricity consumption } (kWh)} \tag{6}$$

where the energy cost is the cost of electricity (as charged per kWh consumption) and demand

charges are charges incurred based on the peak load in kW per month and any other fixed annual charges incurred by the rate plan (e.g., for meters, public goods fees, etc.). The building electricity bill will be determined by the particular tariff structure local to the building’s geographical location. Any on-site fuel costs for building heating such as on-site boilers, water heaters, or furnaces are tracked separately.

In comparison, the fuel cell CHP system has the following costs:

$$\begin{aligned} \text{Cost of electricity } \left(\frac{\$}{kWh} \right) &= f * \text{Cost of } FC \text{ electricity} \\ &+ (1 - f) * \text{Cost of electricity from grid} \end{aligned} \tag{7}$$

where the cost of electricity consists of the levelized cost of electricity provided by the fuel cell system ($LCOE_{FC}$) times the fraction f of electricity consumption provided by the fuel

cell and any cost of electricity that is purchased from the grid if the fuel cell-provided electricity is not sufficient to meet all the electricity demands from the building:

$$\begin{aligned} & \text{Cost of } FC \text{ Electricity } \left(\frac{\$}{kWh} \right) \\ & = LCOE_{FC} = \frac{\text{Installed Cost} * CRF + \text{Annual Maintenance} + \text{Annual Fuel Costs}}{\text{Total electricity provided by FCS } [kWh]} \end{aligned} \quad (8)$$

$$\begin{aligned} & \text{Cost of electricity from grid } \left(\frac{\$}{kWh} \right) \\ & = \frac{\text{Annual energy cost} + \text{Annual demand charges} + \text{Other Charges}}{(\text{Total electricity consumption} - \text{Electricity provided by FCS}) [kWh]} \end{aligned} \quad (9)$$

and

$$\begin{aligned} & LCOE \text{ with } TCO \text{ Credits} \\ & = f * LCOE_{FC} \text{ with } TCO \text{ Credits} \\ & \quad + (1 - f) * \text{Cost of electricity from grid} \end{aligned} \quad (11)$$

CRF = Capital Recovery Factor

$$= \left[\frac{i(1+i)^n}{(1+i)^n - 1} \right] \quad (10) \quad \text{where}$$

The levelized cost of electricity with TCO credits is then defined as follows:

$$\begin{aligned} & LCOE_{FC} \text{ with } TCO \text{ Credits} \\ & = LCOE_{FC} - TCO \text{ Credits} \end{aligned} \quad (12)$$

$$\begin{aligned} & TCO \text{ Credits } \left(\frac{\$}{kWh} \right) \\ & = \frac{(\text{Fuel Savings} + \text{Savings from } CO_2 + \text{Savings from Health and Environment})_{\text{Annual}}}{\text{Electricity provided by FCS } (kWh)} \end{aligned} \quad (13)$$

The method for calculating the savings from health and environmental externalities was discussed above. This approach allocates any fuel savings, savings from CO₂ reductions, and savings from health and environmental externalities to the LCOE of the fuel cell, and the total LCOE with TCO credits is defined as in Eqs. 11 and 12.

In the discussion below, capital costs are drawn from the modeled costs below assuming low-volume production of 100 units per year for 10 kWe and 50 kWe FCS or 1 MWe and 5

annual production, respectively. The LCOE of FC power in this definition includes all of the fuel purchased for FCS operation, but none of the fuel purchased for conventional heating that augments the FCS waste heat utilization.

Other studies have looked at health and environmental benefits of solar and wind [31] where renewable electricity displaces grid electricity. This entry considers CHP which displaces both grid electricity and on-site fuel combustion for heating.

Fuel Cell System Designs and Functional Specifications

PEM Functional Requirements and System Designs

PEM FC system designs and functional specifications have been developed for a range of systems sizes including (1) CHP systems with reformat fuel from 10 to 250 kW_e. These choices are based upon a search of relevant fuel cell literature and patents, industry system spec sheets, as well as industry advisor input.

The choice of these system designs and functional specifications defines the operational parameters for each respective fuel cell system and defines the system components or balance of plant (BOP) that will be the basis for cost estimates. Functional requirements for the stack further define the stack geometries and stack sizing (number of cells per stack) for the DFMA direct manufacturing cost analysis below. The functional specifications also refer to the rated power of the system. Operating at partial load would result in slightly higher efficiency across most of the turndown ratio of the system.

System designs are meant to be “medium fidelity” designs that are representative of actual fuel cell systems to provide the basis for the costing estimates that are the main focus of this entry. As such, this treatment is not scoped with process modeling or optimization of the system design in terms of detailed pressure management, flow rates, or detailed thermal balances. However, the designs are a reasonable starting points for costing based on feedback from industry advisors and for showing key system components, subsystems, and interconnections that are important for understanding system “topography” for analysis and costing purposes.

The systems represented in this entry reflect the authors’ best assessment of existing or planned systems but do not necessarily capture all system components with exact fidelity to existing physical systems, and hence there does not necessarily exist a physical system that is exactly the same as that described here.

PEM System and Component Lifetimes

System and component lifetime assumptions are shown in Table 8 for CHP applications, respectively. These specifications are shared across the system power range for each application. In the application of TCO to a CHP system, overall system life is assumed to be approximately 15 years currently and anticipated to increase to 20 years in the future (2015–2020 time frame). Stack life is 20,000 h in the near term and projected to double to 40,000 h per industry and DOE targets. Subsystem component lifetimes vary from 5 to 10 years, with somewhat longer lifetimes expected in the future compared with the present.

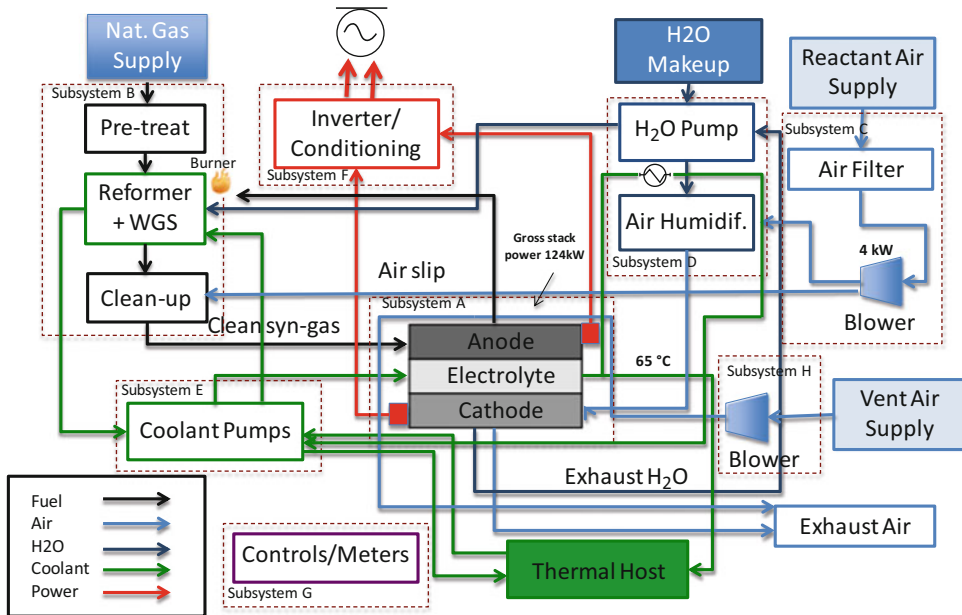
The system turndown ratio is defined as the ratio of the system peak power to its lowest practical operating point (e.g., running at 33 kW_e on a 100 kW_e system is a turndown ratio of 3:1). The stack cooling strategy for all CHP systems is assumed to be liquid water circulation, consistent with CHP system duty cycles and stack lifetime requirements.

PEM CHP System Designs

A representative system design for an PEM fuel cell CHP systems operating on reformat fuel is shown in Fig. 8. Delineation into subsystems is

Fuel Cell Systems: Total Cost of Ownership, Table 8 CHP application common specifications [2]

CHP application – PEM	Near-term	Future (2015–2020)	Units
System life	15	20	Years
Stack life	20,000	40,000	Hours
Reformer life (if app.)	5	10	Years
Compressor/blower life	7.5	10	Years
Water management subsystem life	7.5	10	Years
Battery/startup system life	7.5	10	Years
Turndown ratio	3:1	3:1	Ratio
Expected availability	96	98	Percent
Stack cooling strategy	Liquid	Liquid	Cooling



Fuel Cell Systems: Total Cost of Ownership, Fig. 8 System design for 100 kW PEM CHP system using reformat fuel [2]

provided for modularity of design and also to facilitate the tracking and classification of balance of plant components and costing. The CHP systems are subdivided further into subsystems as follows: (1) fuel cell stack, (2) fuel supply system, (3) air supply, (4) water makeup loop, (5) coolant system, (6) power conditioning, (7) controls and meters, and (8) ventilation air supply.

To improve fuel utilization, the CHP system with reformat fuel has a fuel burner to utilize anode tail gas fuel and also includes an air slip input (approximately 2% concentration) for greater CO tolerance. Note that in some cases where there is not a steady demand for waste heat, there may need to be additional parasitic fans and radiators to dissipate the waste heat.

PEM CHP Functional Specifications

Functional specifications for the 10 kW and 100 CHP systems with reformat fuel are shown in Table 9. These functional specifications were developed based on a variety of industry sources, publically available product specifications, and literature review and include calculated

parameters for stack and system efficiencies for an “internally consistent” set of reference values. A detailed description of the functional specification focused on the 10 kW and 100 system sizes follows below.

The determination of gross system power reflects about 28% overall parasitic power at 10 kW and about 24% at 100 kW, including losses through the inverter. DC to AC inverter efficiency is assumed to be 93% and constant across the system power ranges. Additional parasitic losses are from compressors, blowers, and other parasitic loads and are assumed to be direct DC power losses from the fuel cell stack output power.

The waste heat grade from the coolant system is taken to be 65 °C for all system sizes although a range of other temperatures are possible, mostly over the range of 50–70 °C. The heat exchanger configuration can also depend on the demand temperatures for the heating streams, and the exact cooling and heating loops will be location and system specific. In the use-phase cost model described later in the report, hot water is generated as the main waste heat application with

Fuel Cell Systems: Total Cost of Ownership, Table 9 Functional specifications for CHP fuel cell system operating on reformat fuel [2]

Parameter	CHP system with reformat fuel, 10 kWe	CHP system with reformat fuel, 100 kWe	Unit
Gross system power	12.8	124	kWe
Net system power	10	100	kWe
Electrical output	480 V AC	480 V AC	Volts AC or DC
DC/AC inverter efficiency	93	93	%
Waste heat grade	65	65	Temp. °C
Reformer efficiency	75	75	%
Fuel utilization, overall	90–95	90–95	%
Net electrical efficiency	32	33	% LHV
Thermal efficiency	49	50	% LHV
Total efficiency	81	83	Elect. + thermal (%)
Stack power	12.8	9.5	kWe
Total plate area	360	360	cm ²
CCM coated area	259	259	cm ²
Single-cell active area	220	220	cm ²
Gross cell inactive area	39	39	%
Cell amps	111	111	A
Current density	0.5	0.51	A/cm ²
Reference voltage	0.7	0.7	V
Power density	0.35	0.35	W/cm ²
Single-cell power	77.8	77.9	W

(continued)

Fuel Cell Systems: Total Cost of Ownership, Table 9 (continued)

Parameter	CHP system with reformat fuel, 10 kWe	CHP system with reformat fuel, 100 kWe	Unit
Cells per stack	164	122	Cells
Stacks per system	1	13	Stacks
Parasitic loss	2	16	kWe

enhancement to space heating as an additional possibility. In the reformat fuel case, additional waste heat streams from the anode and cathode exhaust can be routed to the fuel processor reactor burner.

Overall fuel utilization is assumed to be up to 95% for reformat fuel systems with a “single pass” fuel utilization of 80%. This assumes that there is a fuel afterburner in the reformat case.

At the reference cell voltage of 0.7 volts, the net electrical efficiency is 32–33% (LHV) for the reformat systems. These overall electrical efficiency levels are similar to those reported in the literature (e.g., see [32]). Fuel reformer efficiency is estimated to be 75%.

The total overall efficiency of 81–83% is viewed as a benchmark value for the case where a large reservoir of heat demand exists and represents the maximal total efficiency of the system. Actual waste heat utilization and total efficiency will be highly dependent on the site and heating demands. For example, a smaller overall heat efficiency can result if waste heat utilization is confined to building water heating and the building has a relatively low demand for hot water.

There is a well-documented tradeoff of peak power and efficiency. The functional specifications are defined for operation at full-rated power. Moving away from the peak power point to lower current density, the cell voltage increases and thus the stack efficiency improves. Partial load operation has higher efficiency but less power output. For the PEM technology considered here, the system is assumed to be load following, or capable of

ramping its power level up and down to follow electrical demand (to the turndown limit described in Table 8). This system flexibility is an advantage for PEM over higher temperature fuel cell systems and will be included in the use-phase modeling described later in the report.

PEM Cell Stack Sizing

Total fuel cell plate area is taken to be 363 cm² based on inferences and interpretation of publically available industry spec sheets (All functional specifications (e.g., gross and net system power, cell sizes, stack current density, etc.) are based on inferences and interpretations of publically available data, patents, and literature by members of the research team from LBNL and UC-Berkeley and should not be interpreted as actual product data from any other fuel cell stacks or component vendors.). Catalyst-coated membrane area is about 72% of this area due to plate border regions and manifold openings. Single-cell active area has an additional 15% area loss. As described further in the DFMA costing section below, this is due to the overlap and alignment area loss associated with the frame sealing process. The tradeoff here is a longer anticipated frame lifetime (20,000 h) and higher reliability from this frame sealing process for continuous power applications versus the lower area loss with an alternative edge sealing process.

SOFC System and Component Lifetimes

System and component lifetime assumptions for SOFC CHP systems are shown in Table 10. These specifications are shared across the system power

range for each application. Overall system life is assumed to be approximately 15 years currently and anticipated to increase to 20 years in the future (2015–2020 time frame). Stack life is assumed to be 20,000 h in the near term and projected to double to 40,000 h per industry and DOE targets. Subsystem component lifetimes are assumed to vary from 5 to 10 years, with longer lifetimes around 20 years expected in the future. Direct air and off-gas cooling strategy is utilized for stack cooling for cost savings and BOP design specifications.

System Design and Functional Specifications for SOFC CHP Systems

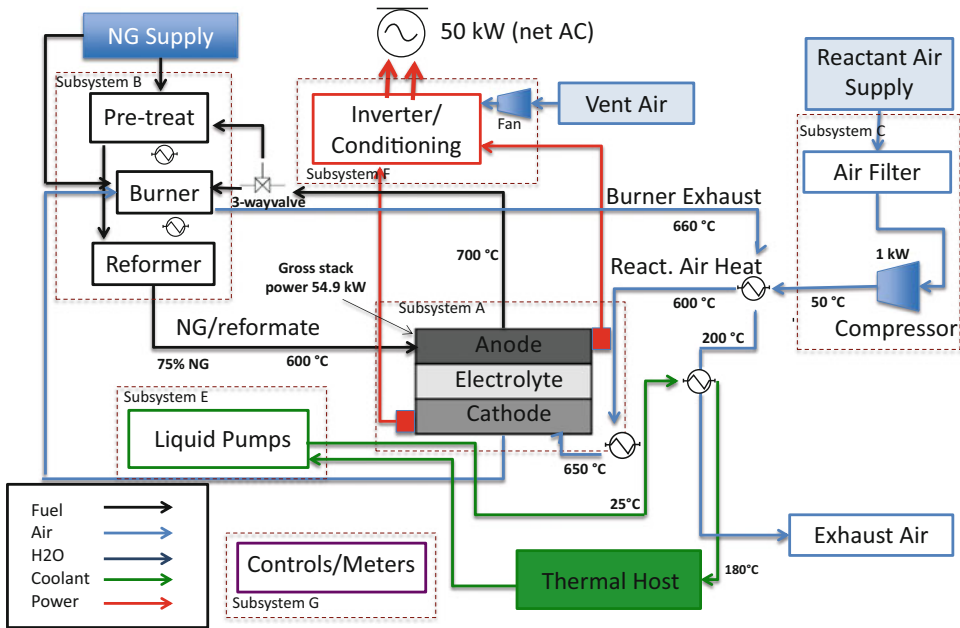
System designs for both a SOFC CHP operating on reformat fuel will be discussed in this section. System design rationale and operations will be discussed in greater detail.

Figure 9 shows the system design for a SOFC CHP system operating on reformat fuel. Delineation into subsystems is provided for modularity of design and also to facilitate the tracking and classification of balance of plant components and costing. Similar to the PEM case above, the CHP systems are subdivided further into subsystems as follows: (1) fuel cell stack, (2) fuel supply system, (3) water recirculation, (4) power conditioning, (5) coolant subsystem, and (6) controls and meters.

Functional specifications for the 10 and 50 kWe CHP systems with reformat fuel are shown in Table 11. These functional specifications were developed based on a variety of

Fuel Cell Systems: Total Cost of Ownership, Table 10 Specifications and assumptions for SOFC CHP system [3]

CHP application – SOFC	Near-term	Future	
System life	15	20	Years
Stack life	20,000	40,000	Hours
Reformer life (if app.)	5	10	Years
Compressor/blower life	7.5	10	Years
Water management subsystem life	7.5	10	Years
Battery/start-up system life	7.5	10	Years
Turndown % (>50 kW)	0	25	Percent
Turndown % (<50 kW)	25	50	Percent
Expected availability	96	98	Percent
Stack cooling strategy	Air + off-gas	Air + off-gas	Cooling



Fuel Cell Systems: Total Cost of Ownership, Fig. 9 SOFC CHP system design schematic for 50 kW CHP system [3]

industry sources and literature and include calculated parameters for stack and system efficiencies for an “internally consistent” set of reference values. A detailed description of the functional specification focused on the 10 and 50 kWe system sizes follows below. The determination of gross system power reflects about 10% overall parasitic power at 10 kWe and about 9.7% at 100 kWe, including losses through the inverter. DC to AC inverter efficiency is assumed to be 95% and constant across the system power ranges. Additional parasitic losses are from compressors, blowers, and other parasitic loads and are assumed to be direct DC power losses from the fuel cell stack output power.

The waste heat grade from the coolant system is taken to be 220 °C for all system sizes although a range of other temperatures are possible, mostly over the range of 50–70 °C. The heat exchanger configuration can also depend on the demand temperatures for the heating streams, and the exact cooling and heating loops will be location and system specific. In the use-phase cost model described later in the report, hot water and space heating are generated as the

main waste heat application with enhancement to absorption chilling as an additional possibility. Additional waste heat streams from the anode and cathode exhaust can be routed to the fuel processor reactor burner.

At the reference cell voltage of 0.8 volts, the net electrical efficiency is 59% (lower heating value, or LHV) for the reformat systems. These overall electrical efficiency levels are similar to those reported in the literature [11]. The total overall CHP system efficiency of 84% is viewed as a benchmark value for the case where a large reservoir of heat demand exists and represents the maximal total efficiency of the system. Actual waste heat utilization and total efficiency will be highly dependent on the site and heating demands. For example, a smaller overall heat efficiency can result if waste heat utilization is confined to building water heating and the building has a relatively low demand for hot water.

Total fuel cell plate area is taken to be 540 cm². Active catalyzed area is about 61% of this area due to plate border regions and manifold openings, and single-cell active area has an additional 10% area loss due to the frame sealing process.

Fuel Cell Systems: Total Cost of Ownership, Table 11 Functional specifications for CHP system operating on reformat fuel [3]

Parameter	10 kWe CHP system reformat fuel	50 kWe CHP system with reformat fuel	Units
Gross system power	11.0	54.9	kW DC
Net system power	10	50	kW AC
Electrical output	220 V AC	480 V AC	Volts AC or DC
DC/AC inverter efficiency	95	95	%
Waste heat grade	220	220	Temp. °C
Fuel utilization % (overall)	N/A	N/A	%
Net electrical efficiency	59	59	% LHV
Thermal efficiency	24	24	% LHV
Total efficiency	84	84	Elect. + thermal (%)
Stack power	11.0	54.9	kW
Total plate area	540	540	cm ²
Actively catalyzed area	329	329	cm ²
Single-cell active area	299	299	cm ²
Gross cell inactive area	45	45	%
Cell amps	105	105	A
Current density	0.35	0.35	A/cm ²
Reference voltage	0.8	0.8	V
Power density	0.28	0.28	W/cm ²
Single-cell power	84	84	W
Cells per stack	130	130	Cells
Stacks per system	1	5	Stacks
Parasitic loss	0.5	2.5	kW AC

The 10 kWe system consists of 130 cells in a single stack, while the 50 kW system has 5 stacks of 130 cells each.

Total Cost of Ownership Modeling Results

PEM Fuel Cell System Manufacturing Costs

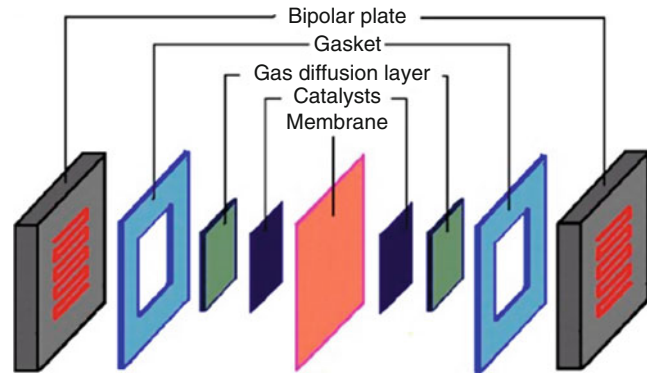
A PEM unit cell consisting of bipolar plate/gasket/GDL/CCM/GDL/gasket is shown in Fig. 10 where the gasket represents the cell frame/seal. Many sequential cells assembled together form a fuel cell stack. Typically the stack is assembled with some compression mechanism such as tie rods or compression bands with conductive endplates on both sides of the stack.

For this entry, bottom-up cost analysis is done for each of the critical stack cost components, namely, the catalyst-coated membrane (CCM), gas diffusion layer (GDL), MEA frame/seal, bipolar plate (BPP), and stack assembly. Details of process costing can be found in Wei et al. [2]. To illustrate the bottom-up analysis, a more detailed discussion for two key process modules is provided: the catalyst-coated membrane and bipolar plates. The cost critical bill of materials is shown in Table 12.

Component process yield is assumed between 60% and 99.5%, line availability between 85% and 95%, and daily setup time between 60 and 5 min. All are scaled with production volume and range from current values to achievable future values. These assumptions have been obtained through consultation with industry sources including Ballard Power Systems and assessment of the current published literature. Yield, availability, and setup time differs from module to module due to differences of the manufacturing processes, difficulties handling the different materials, and embedded value of the product further down the manufacturing line. The process yield assumption represents an intermediate value between the very high-yield assumptions in [7] and the low-yield assumptions of 60% to 70% in ACI Technologies [33] and explicitly assumes that the yield is dependent on the production volume. Implicit in this assumption is

Fuel Cell Systems: Total Cost of Ownership,

Fig. 10 Schematic of PEM fuel cell unit



Fuel Cell Systems: Total Cost of Ownership, Table 12 Key bill of materials for stack manufacturing

Material	Component	Cost	Reference
Teflon perfluoroalkoxy (PFA) film	CCM	\$9.78 m ⁻²	Professional plastics
Platinum	CCM	\$1402 troy ounce ⁻¹	Richest group, Shanghai, China
Carbon fiber	GDL	\$9.50–9.72 m ⁻²	Sinha [8]
Polytetrafluorethylene (PTFE)	GDL	\$22.17 kg ⁻¹	Sinha [8]
Polypropylene	Carbon BPP	\$1.597 kg ⁻¹	2011 Market price
Graphite	Carbon BPP	\$6.761 kg ⁻¹	2011 Market price
Carbon black	Carbon BPP	\$6.35 kg ⁻¹	2013 Market price
Carbon epoxy	Carbon BPP	\$97.38 L ⁻¹	Eccobond 60 L
SS316L	Metal BPP	\$4 kg ⁻¹	James et al. [7]
Chromium nitride (CrN)	Metal BPP	\$50 kg ⁻¹	
Polyethylene naphthalate (PEN)	Frame/seal	\$5 kg ⁻¹	CES 2012 ^a
Fluorinated ethylene propylene (FEP)	Frame/seal	\$10 kg ⁻¹	CES 2012 ^a

^aCES 2012: *Cambridge Engineering Selector* computer software. Vers. 2012. Cambridge, UK: Granta Design Ltd., 1999

that “learning-by-doing” leads to higher yield at higher production volumes. Note that the process yield assumed here is the total yield for an individual stack component, not the overall stack yield nor the step by step yield breakdown. Table 13 shows this breakdown. Furthermore, multiple production lines are considered for tooling optimization of low- and high-volume production.

Catalyst-Coated Membrane

For this entry, a decal transfer coating process is adopted as a base flow with coating lines for cathode and anode catalyst followed by a

lamination step to combine the two layers to form a catalyst-coated membrane (CCM), all using automated roll-to-roll or web line processing. The flow is similar in concept and materials to US Patent 20090169950 [34].

Slot die coating was chosen as a representative process for catalyst ink deposition since it is a mature technology with a high degree of process control capability in high-volume manufacturing. This approach has been demonstrated for other thin film products and is expected to be able to scale up to larger volumes for the catalyst coating operation. Other deposition techniques could be used such as spray coating, gravure, roll coating,

etc., but were not explored. Ultra-low catalyst loading, e.g., nanostructured thin films, is not required for longer lifetime stationary applications where a higher loading can be amortized over a longer amount of time. On the down side, wet deposition manufacturing issues include the management of volatile and/or explosive solvents for safety and environmental control, wet mixing control of viscosity, particle uniformity, and management of plumbing lines and concentration gradients.

For the slot die coating, catalyst ink is mixed in a tank and extruded through the slot die coater. Following deposition, the coated membrane or backing layer passes through an IR drying oven to bake off the ink solvents. Anode-side and cathode-side catalyst deposition is done on separate lines due to swelling issues during drying and product quality and process control difficulties with concurrent or serial deposition. Anode and cathode layers are pressed together in a heated nip roller to form the final CCM product.

The overall deposition area is enclosed in a clean room environment at Class 1000 to control for contaminants and particles. An inspection is done after each deposition and thermal treatment pass. Fume hoods to thermal oxidizers are employed to control volatile organic compound (VOC), CO, and volatile hazardous air pollutant (HAP) emissions. Overall, both tooling lines (high volume and low volume) and equipment configuration have been validated by both industry advisors and vendor inputs.

The CCM membrane is a Nafion membrane from DuPont with 25.4 μm thickness and is assumed to be a purchased part. The decision to purchase the membrane was based on industry input, the cost and complexity to bring up a membrane manufacturing line, and the fact that Nafion is readily available and is expected to scale in price with higher demand from increasing PEM fuel cell production. Cathode and anode Pt loading are assumed to be 0.4 and 0.1 mg cm^{-2} , respectively. This loading is similar to that assumed in [33] and Pt loading and price is also a key variable for the sensitivity analysis later in this entry.

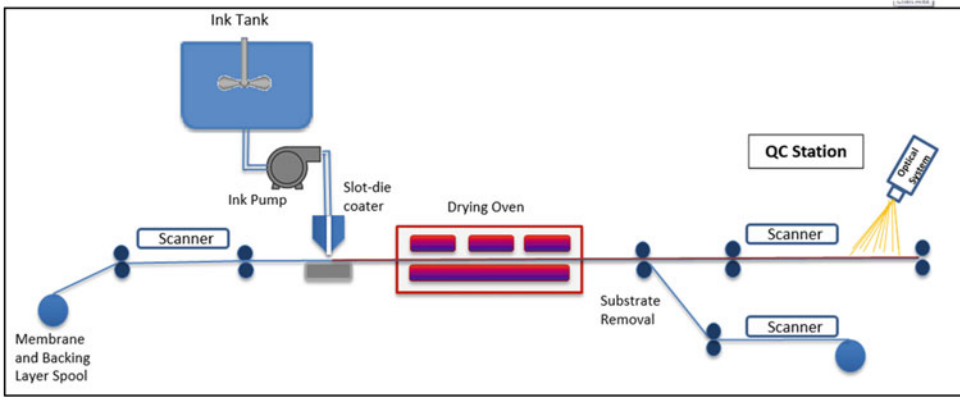
The CCM is made from depositing a catalyst layer (cathode) over a Nafion membrane and depositing an anode layer over Teflon paper then attaching these two layers via a lamination process. Teflon PFA paper is used as a substrate in the decal transfer method for the deposited anode and is then attached to the coated membrane (which was previously coated on one side) to form the final CCM (Fig. 11).

Bipolar Plates

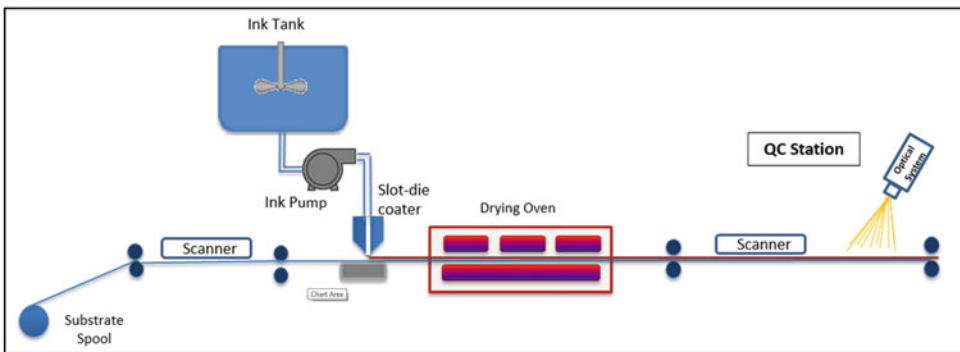
Bipolar plates are conductive plates in the fuel cell stack which separate MEAs and act as an anode for one MEA cell and a cathode for the next cell. Bipolar plates are usually made from metal, carbon, or conductive composite polymer (usually incorporating carbon). Bipolar plates have a number of functions within the fuel cell stack including separating gases between cells, providing a conductive medium between the anode and cathode, providing a flow field channel for the reaction gases, acting as a solid structure for the stack, and transferring heat out of the cell.

Typically, fuel cell plate vendors/developers have used compression molding where resin or polymer materials are blended with conductive filler material or embossing GRAFOIL[®] flexible graphite where graphitic carbon is impregnated with resin. Often, thermal treatment is done after molding to completely cure the material and/or to reduce volatile organic compound (VOC) content. Recently metal plates have also been considered, particularly in the automotive applications; however, a less established plate lifetime (about 5000–6000 h) suggests that using more standard graphite composite-based plates is a more durable option.

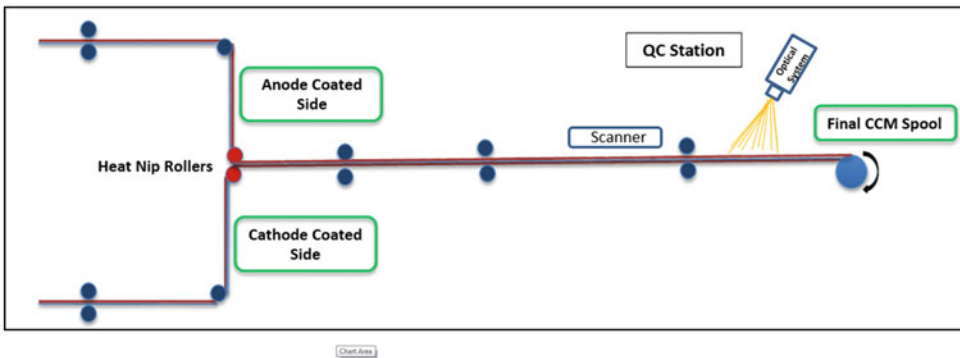
Injection molding is better suited to high-volume manufacturing than compression molding as it offers lower cycle times and established process technology with good dimensional control. However, material issues can make injection molding challenging for fuel cell applications. For example, conductive filler is needed for better conductivity, which adds to material costs and makes the technique more difficult due to higher viscosity and poorly controlled melt properties.



(a) Cathode-side



(b) Anode-side



(c) Final CCM

Fuel Cell Systems: Total Cost of Ownership, Fig. 11 Schematic diagram for roll-to-roll coating line: (a) cathode line, (b) anode line, and (c) final product

As plates get larger in area, tolerances and control of plate planarity and flatness become larger concerns and need to be evaluated for injection molding. Additionally, plate brittleness can lead to cracking, and therefore plates may need added thickness, which results in undesirable

volume and weight. Nonetheless, recent work from the Center for Fuel Cell Technology (ZBT) at the University of Duisburg-Essen (see, e.g., [35, 36]) has achieved injection molded plates with good electrical and physical performance with a slight increase in plate thickness (2 mm).

As noted in Yeetsorn [37], research and development is needed for better composite materials with maximal electrical conductivity. One cited pathway is the development of more advanced materials with the proper conductive network structure. Here, an analysis of injection molded plates is presented for cost comparison with metal plates. Injection molding was modeled instead of compression molding since this entry is targeted for higher volume and injection molding is expected to yield lower costs.

This implicitly assumes that continued development will occur in composite materials with conductive fillers, potentially including nano-structured materials that will allow injection molding to be viably employed. Stationary applications allow for slightly thicker plates since volume and weight are not as stringent concerns as that for the automotive application. Slightly thicker plates may also achieve better quality in terms of dimensional tolerances, plate stability, and yield.

Injection Molded Carbon Plates

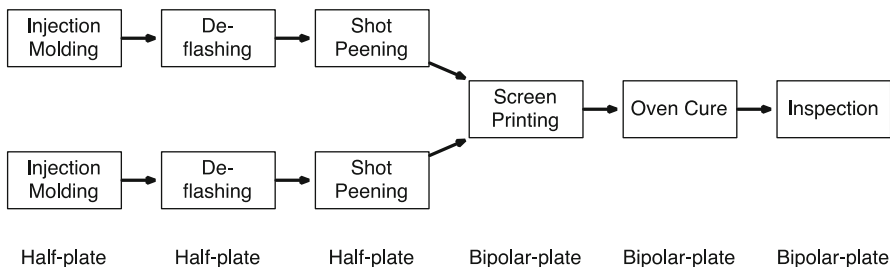
The process flow is shown in Fig. 12. It is assumed that the input material (composite) is already mixed and pelletized. Injection molding machine size, electrical power, and cycle time are determined by a model created by Laboratory of Manufacturing and Sustainability at University of California, Berkeley [38], that results in cycle times estimated to be 30.6 s per half plate (half of a bipolar plate) in a lower-volume configuration and 16.1 s with a higher batch size and two injection cavities. Injection molding is followed by a deflashing (removal of unwanted excess material) and shot peening step. The shot peening

step treats the surface to reduce gas permeability and become a slightly compressive layer. This step is in lieu of a separate resin-curing step typically used to treat the surface. A screen printer is used to coat epoxy on the half plates to form bipolar plates. This is followed by an oven curing step and then a final inspection. Potential plate cleaning steps could also be envisioned and would add to the cost but were not included in this entry due to the uncertainty in cleaning requirements.

Plate materials are assumed to be a combination of polypropylene binder with a mixture of graphite and carbon black conductive filler. Equipment costs are fairly evenly distributed between process modules with the injection molding machine the largest capital cost.

Manufacturing cost is typically high at low production volumes, and therefore individual components would be purchased rather than manufactured in-house. However, it is assumed that all components are manufactured in-house (with exception to the components specifically mentioned in the method section). For this reason, the cost reduction is larger when transitioning from low to high volumes than if there were more purchased components at low-volume production.

Individual component cost breakdowns in $\$/\text{kW}^{-1}$ for 100 kW CHP reformate fuel cells are shown in Fig. 13 for the CCM and bipolar plates. The CCM cost is dominated by direct material cost at all production volumes due to the high cost of the platinum catalyst. Other modules such as the GDL and assembly also have very high material cost at high production volumes. This is due to high processing manufacturing



Fuel Cell Systems: Total Cost of Ownership, Fig. 12 Process flow of bipolar plate manufacturing

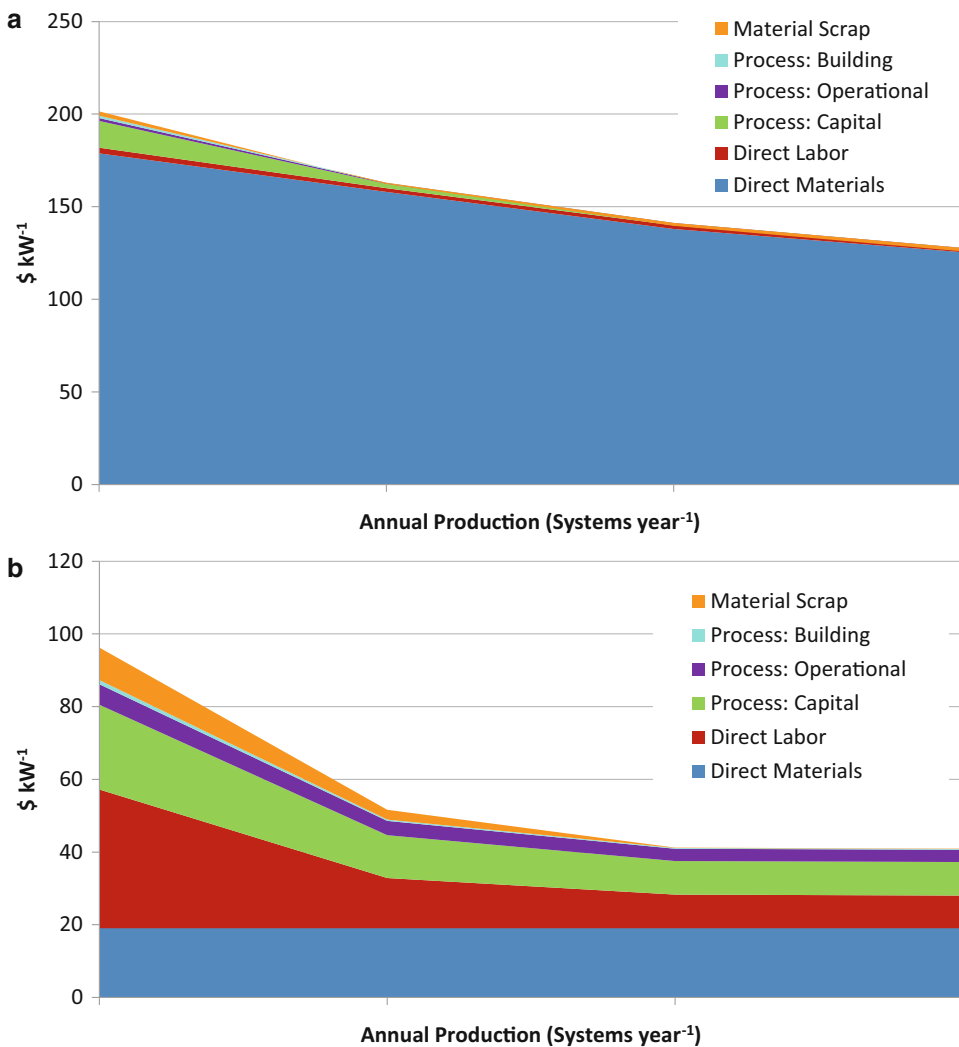
with high line utilization. Also, scrap cost is high for the frame/seal due to high material losses when cutting out the cell sized slot.

PEM Stack Direct Manufacturing Costs

Direct stack manufacturing cost vs. annual production volume is shown in Table 14 for CHP systems with reformat fuel and backup power systems, respectively. This provides an indication of future potential PEM fuel cell stack costs with continued process automation, economies of scale, and learning by doing. When production

volume is increased, the stack cost decreases considerably.

Two breakdowns of cost components are shown in Figs. 14 and 15 for a 50 kW system. Figure 14 shows that the CCM is largest cost driver of the stack in part due to the high catalyst cost across process volumes followed by the bipolar plates and the GDL. Figure 15 shows that direct materials and capital costs are the largest cost components at low volume and direct materials dominate costs at higher volumes.

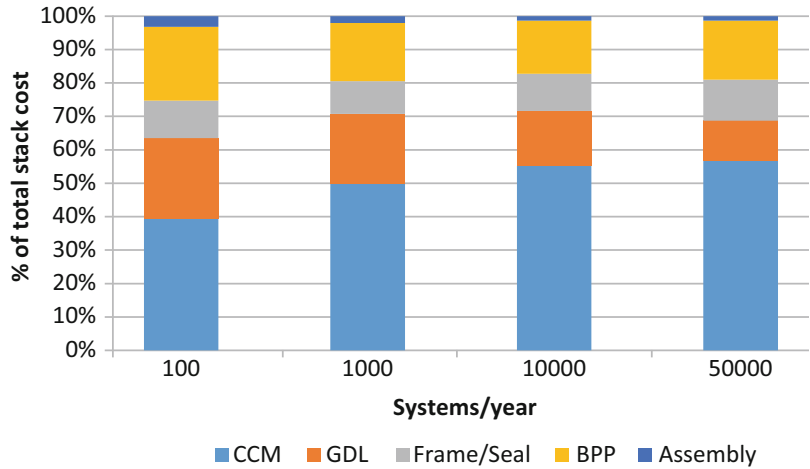


Fuel Cell Systems: Total Cost of Ownership, Fig. 13 Component cost breakdown of 100 kW CHP(\$ kW⁻¹) for (a) catalyst-coated membrane and (b) bipolar plate

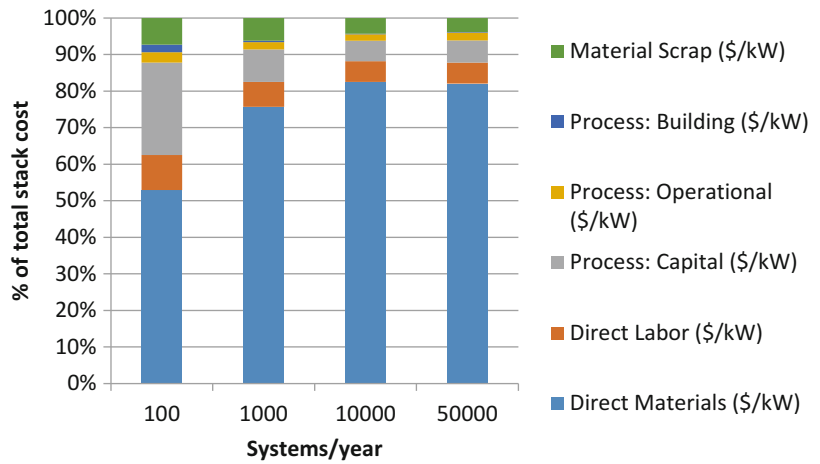
Fuel Cell Systems: Total Cost of Ownership, Table 14 Stack cost estimate in (\$/kWe) as a function of annual manufacturing volume

System size (kWe)	100 systems/yr	1000 systems/yr	10,000 systems/yr	50,000 systems/yr
10	1340	497	333	284
50	596	352	272	239
100	466	313	249	219
250	377	279	231	203

Fuel Cell Systems: Total Cost of Ownership, Fig. 14 Disaggregation of stack cost by relative percentage of stack components cost to overall stack cost for 50 kWe systems



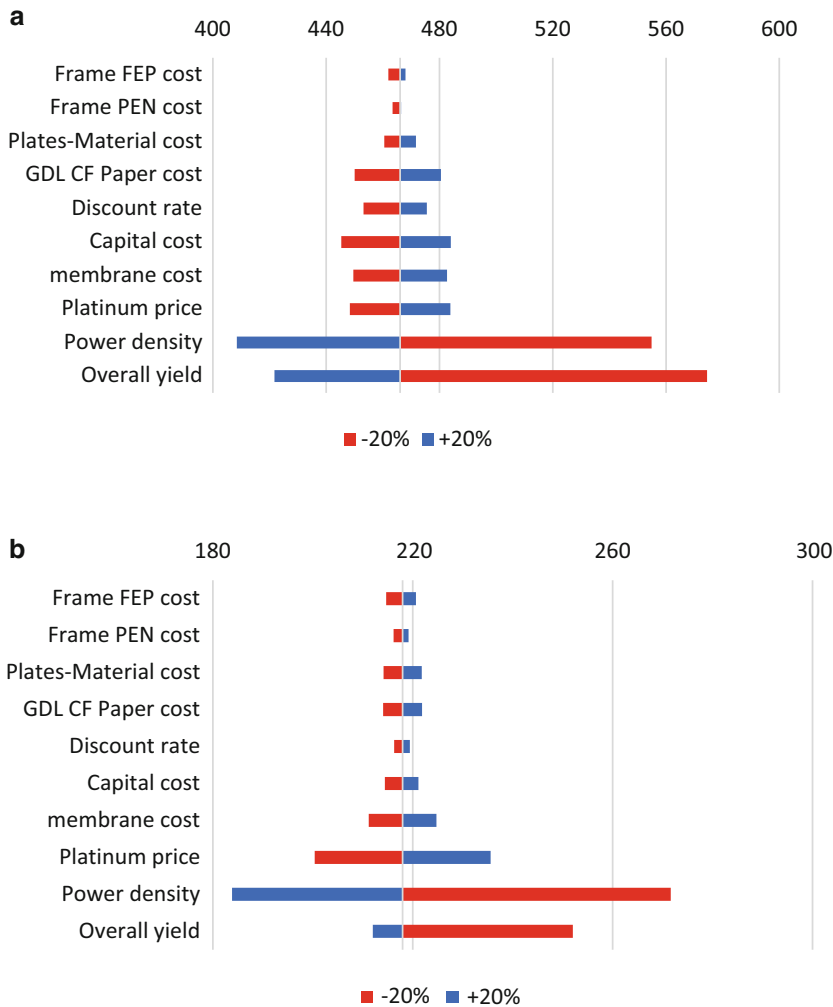
Fuel Cell Systems: Total Cost of Ownership, Fig. 15 Disaggregation of stack cost by relative percentage of cost components to overall stack cost for 50 kWe systems



PEM Stack Cost Sensitivity Analysis

A sensitivity analysis at the stack level is presented in this section for 100 kW systems at different production volumes (as shown in Fig. 16). The impact to the stack cost in \$ kW⁻¹ is calculated for a ±20% change in the sensitivity parameter being varied.

As it can be seen from these plots, module process yield and power density are the most sensitive cost assumptions. Pt price and Nafion membrane price are among other important factors. This is not surprising for expensive materials and since from the above discussion, material costs dominate at high production volumes. The



Fuel Cell Systems: Total Cost of Ownership, Fig. 16 Sensitivity analysis for 100 kW stack manufacturing parameters at different production volumes: (a)

100 systems per year⁻¹ and (b) 50,000 systems per year⁻¹ (Note: upper bound for yield is 100% and lower bound varies between low and high production volumes)

discount rate and capital cost are not large factors at high volume since material costs dominate the overall cost. Note that yield becomes less sensitive at high volume for two reasons: (1) overall yield is assumed to be very high at high volume ($\geq 95\%$), and (2) material costs dominate at high volume and a significant portion of material costs are recovered from rejected material.

1. Fuel subsystem
2. Air subsystem
3. Coolant subsystem and humidification subsystems
4. Power subsystem
5. Control and meter subsystem
6. Miscellaneous subsystem

PEM Fuel Cell CHP Balance of Plant and System Costs

To facilitate the analysis, the BOP is divided into six subsystems or subareas listed below:

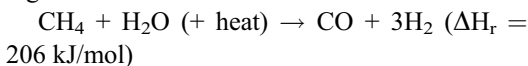
For each subsystem, a detailed list of components and component sizing is generated based on the system design. Subsystem components are estimated using bottom-up system design, component sizing, and vendor discussions. Cost

estimates are based on the cost estimates from publically available sources such as online price quotes or direct quotes from material or component vendors. More details can be found in Wei et al. [2].

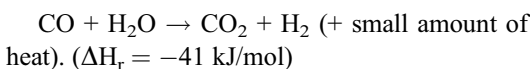
The BOP includes items such as valves, compressors, pumps, wiring, piping, meters, controls, etc. that are associated with the complete operation of the fuel cell system. Six major areas make up the BOP and are shown in Fig. 8. With reference to this figure, the plant is fed by natural gas where it is reformed, shifted, and purified in the reformer to a CO-free hydrogen-rich reformat fuel before entering the stack. The hydrogen-rich fuel enters the anode, and the compressed air enters the cathode side to generate DC electricity in the PEM stack. The generated power is converted to AC power through an inverter for load usage. A coolant loop circulates around the stack for cooling purpose. Thermal power is recovered from the stack and fuel burner for CHP applications. A blower generates vent atmospheric air to cool the stack. Each of the subsystems are listed and described in greater detail in the section below.

Fuel Processing Subsystem

The fuel processing subsystem is comprised of components associated with the operation of the fuel reforming process. The purpose of the fuel processor is to convert a hydrocarbon fuel (e.g., natural gas) into a hydrogen-rich gas via steam-methane reforming. In steam-methane reforming, natural gas reacts with steam in the presence of heat to produce hydrogen, carbon monoxide, and a small amount of carbon dioxide via the following chemical reaction:



Subsequently, steam and carbon monoxide are reacted using a catalyst to produce carbon dioxide and additional hydrogen. The reaction is exothermic and is called the water-gas shift reaction:



After that, carbon dioxide and other impurities are then removed from the reformed gas stream.

The cleaned fuel is fed into the fuel cell anode via a piping system that is controlled with manifolds and valves. Additional components include gas sensors for hydrogen level detection throughout the system.

Air Subsystem

The air subsystem consists of components associated with oxidant delivery to the fuel cell stack. Air supply from the atmosphere undergoes cleanup with an air filter and is pressurized with a blower. The air is humidified before entering the cathode. In addition, a fan unit takes in vent air for the purpose of stack cooling. Additional components such as piping, manifolds, and valves are employed for air delivery into the fuel cell stack. Gas sensors are also used to monitor oxidant levels throughout the system.

Coolant and Humidification Subsystem

The coolant subsystem consists of components associated with water management in the FCS, including cooling of the fuel cell stack. Water coolant from the coolant tank is cooled with a heat exchanger and recirculated through the stack via a pump unit.

Thermal Management Subsystem

For CHP operation, the exhaust heat from the burner unit and the fuel cell stack can be utilized to provide both water and space heating (thermal host) through the use of a liquid-liquid and gas-liquid heat exchangers. In order to obtain the costs of the heat exchanger used in the CHP FCS to recover the waste heat, the maximum heat from the fuel cell was calculated using the thermal and electrical efficiencies from the functional specs described above. Using the value, the required heat exchange area was evaluated using the log mean temperature difference method [39], where the required temperatures were obtained from this entry's design specifications. Using the computed areas, the costs of the heat exchangers were computed for both brazed plate and bolted heat exchangers with cost functions available from online database [40].

Power Subsystem

The power subsystem includes equipment for power inversion (from direct or “DC” current to “alternating” or AC current) and power regulation. In order for fuel cells to deliver power at the required voltage, a DC-DC converter is used to regulate fluctuating DC fuel cell voltage input to a specified voltage output, particularly for direct DC backup power applications. For most stationary FC applications, the fuel cell will be connected to the electricity grid where AC power is required for residential or utility power. An inverter is necessary for converting the DC power provided by a fuel cell to AC power, and an additional DC-DC converter may or may not be needed depending on the system design and the characteristics of the inverter. A transistor and a transformer were included in the subsystem to account for voltage fluctuations in the cell for the purposes of voltage and current conversions (step-up/step-down) to help meet the fluctuating electrical demands from the facility. Additional components for the working operation of the power subsystem include relays, switches, fuses, resistors, and cables.

Control and Meter Subsystem

The control and meter subsystem contains system control-related components for system operation and equipment monitoring. During a fuel cell system’s operation, variables such as flow rates, power output, temperature, and cooling need to be controlled. Sensors, meters, and pressure gauges are used for system monitoring of these variables. A variable frequency drive (VFD) is used to control the system’s actuation units, which include regulation of valves, pumps, switches, etc. A central processing unit (CPU) acts as the primary controller of the system, keeping the fuel cell system operating at the specified condition by monitoring the interaction between the monitoring sensors and actuating parts.

Miscellaneous Subsystem

The miscellaneous subsystem comprises external items outside of the stack that provides support, structure, and protection for the FCS. Items included in this subsystem are system enclosure,

fire safety panels, fasteners, tubing, and system assembly labor.

Table 15 shows component and subsystem costs of 10 and 100 kW CHP 100 at 1000 units per year, and Table 16 has a summary of BOP costs for PEM CHP.

The total direct system costs (stack plus BOP) are shown in Fig. 17. Total costs are seen to drop by about 20% for every factor of 10 increase in volume for a given system size, while increasing

Fuel Cell Systems: Total Cost of Ownership, Table 15 Component and subsystem cost of 10 and 100 kW CHP reformate system at 1000 units per year annual volume

CHP system with reformate fuel component breakdown (for 1000 systems/year)	\$/kW	
System size	10 kW	100 kW
Fuel processing subsystem		
Integrated concentric-shell reformer for reforming natural gas	602	231
Air subsystem		
Air tank, humidification pump, air pump compressor, radiator, manifolds, air piping	246	59
Coolant subsystem		
Coolant tank, pump, coolant piping, external cooling motor	105	59
Thermal management subsystem		
Liquid-liquid heat exchanger, gas-liquid heat exchanger, condenser	182	76
Power system		
Power inverter, braking transistors, transformer, power supply, relays, switches, fuses, bleed resistor, Ethernet switch, power cables, voltage transducer	421	249
Control/meter subsystem		
Variable frequency drive, thermostats, central processing unit, flow sensors, pressure transducer, temperature sensors, hydrogen sensors, sensor heads, virtual private network	231	66
Miscellaneous subsystem		
Tubing, wiring, enclosure, fasteners, fire detection panel, safety leak detection system, ISO containers, labor	390	154
Total in \$/kW	2177	894

Fuel processor subsystem costs were adopted from earlier work by Strategic Analysis Inc. [16]

the system size from 10 to 100 kW results in about 50% lower cost. Note that customer purchase price would be higher than these direct costs, depending on the corporate markup for general and administrative costs, sales and marketing, research and development, installation costs, and any other fees and costs (insurance, warranties). A 50% corporate markup and a nominal 33% additional cost for installation are assumed, and any additional fees and costs, for a customer cost which is approximately double those shown in Fig. 17. For example, the externality modeling below utilizes a 50 kWe system, and a customer cost of \$4000/kWe is estimated at an annual production of 100 units per year.

PEM Fuel Cell CHP System Life-Cycle Cost and LCIA Model Example

This section describes the TCO model output for PEM CHP systems in the example commercial building case of a small hotel. More examples of LCIA by building type are provided in [2, 3]. Here, an illustrative example under two

assumptions is provided: a static electricity grid and an evolving electricity grid that is getting progressively cleaner in both carbon and criteria emissions.

Figure 18 shows the externality benefits for six cities for a 50 kW CHP system in a small hotel. These values are found using the methodology shown in Fig. 5 using two different sets of marginal emission factors: those from Siler Evans et al. [24] for large area NERC regions and eGRID subregions [21] and AP2 damage factors in Tables 4 and 5. The average value of externality benefits is fairly well matched in Phoenix, Minneapolis, and Chicago, but is less well matched for New York City and Houston. The average across all six cities is reasonably well matched however. The largest benefits are in the two Midwestern cities, Minneapolis and Chicago, and are dominated by health and environmental savings, driven by the larger electricity grid emission factor in those two locations.

Example output of the LCC and LCIA model for a 50 kW small hotel in five representative cities

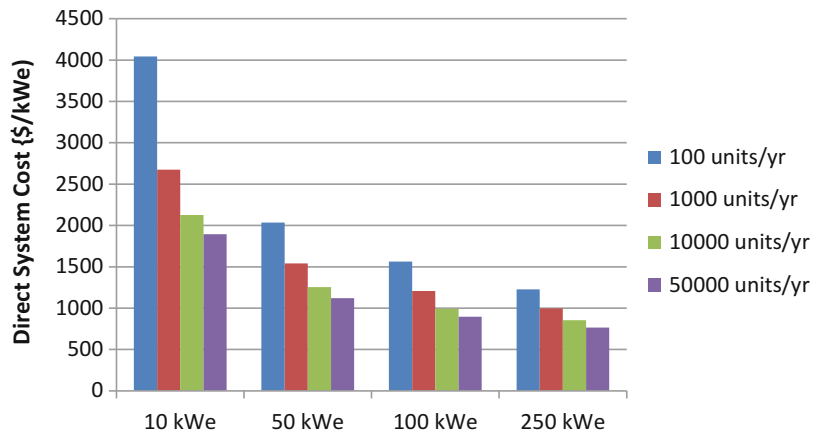
Fuel Cell Systems: Total Cost of Ownership,

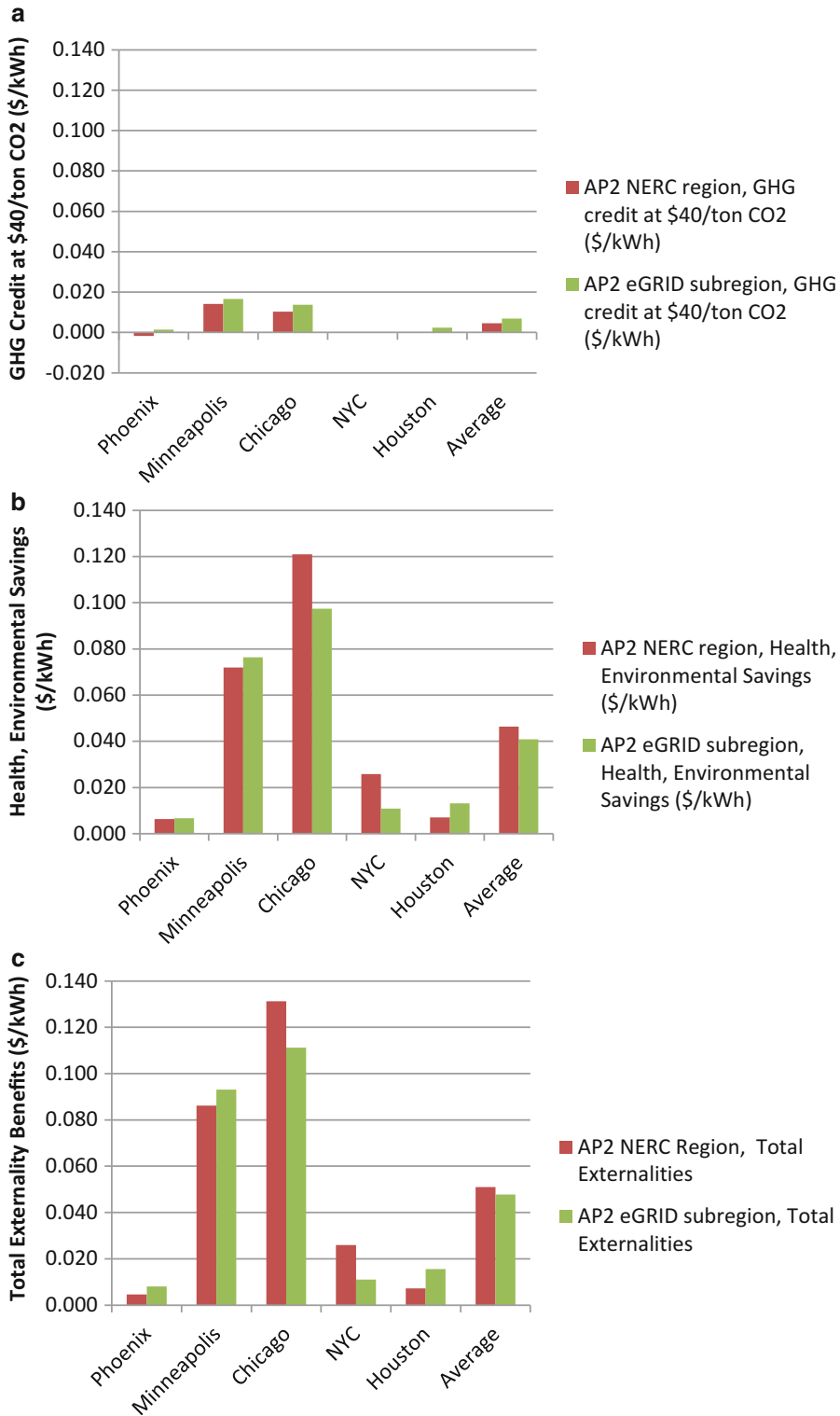
Table 16 Summary of BOP cost in \$/kW for CHP systems with reformat fuel [2]

System size	Units per year			
	100	1000	10,000	50,000
10 kW	2703	2177	1792	1612
50 kW	1439	1188	982	881
100 kW	1097	894	744	676
250 kW	852	719	622	562

Fuel Cell Systems: Total Cost of Ownership,

Fig. 17 Direct costs for PEM CHP systems as a function of system size and manufacturing volume





Fuel Cell Systems: Total Cost of Ownership, Fig. 18 Total externality benefits for a 50 kWe PEM CHP system in a small hotel using AP2 health and

environmental impact model and either NERC region marginal emission factors (Siler Evans et al.) [24] or eGRID subregion emission factors (EPA) [21]

is shown in Table 14. From Fig. 17, a customer cost of \$4000/kWe is assumed or about double the direct system cost at an annual manufacturing volume of 100 systems per year.

The cost of electricity in 2015 is shown in Fig. 19 for the case of a 50 kW PEM fuel cell system in a small hotel at an installed cost of \$4000/kWe. The first bar is the reference cost of electricity for the reference case of no fuel cell system in a 50 kW small hotel; the second bar is the LCOE from the fuel cell system. The third and fourth bars are the reduction in FC LCOE with heating fuel savings and then with health and environmental savings. The final bar is the LCOE with TCO savings for the fuel cell system case with electricity from the fuel cell system and with any purchased electricity from the grid. There is a net reduction in electricity cost in Minneapolis and Chicago which is driven by the health and environmental externality savings (Table 17).

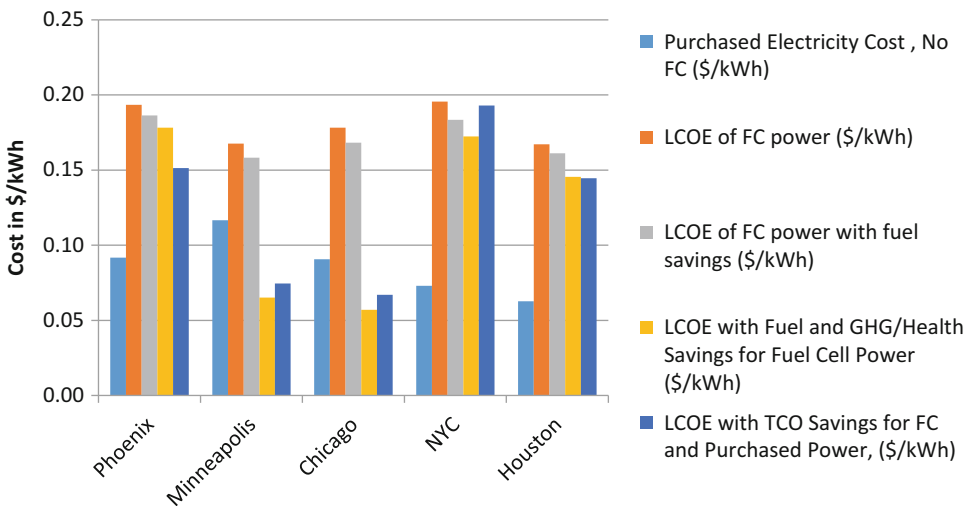
The estimated cost of electricity in 2030 with the estimated future grid emission reductions as described in section “Life-Cycle Impact Assessment Modeling” is shown in Fig. 20 with the same sequence of costs as in Fig. 19. In all cases the LCOE with TCO savings for FC and purchased power is greater than the cost of electricity in the reference case without a fuel cell system.

Cash Flow with Static and Lower Emissions from Electricity Grid

Another view of this is the consideration of cash flow. In this depiction, the capital costs are taken in the first year, and from this initial outlay, the annual difference in operating and fuel costs for a fuel cell system vs. the reference case of no FCS is added. Without externalities and assuming a static case of fixed fuel cell and grid emission factors, the private cash flow is negative for all years since the fuel cell system has higher annual cost for each year of operation.

Figure 21 shows a “societal cash flow” with both private costs and social costs including externalities. This depicts the overall costs to the private owner and to society. Note that this is a notional cash flow since the benefits that accrue to society are not captured by a private entity. In this case, because there is a roughly \$29,000 TCO savings per year (Note that the LCOE with TCO savings above includes the annualized capital costs of the fuel cell system but that the cash flow cash flow treats all equipment cost as an initial cash outlay.), the net cash flow is very favorable after 15 years.

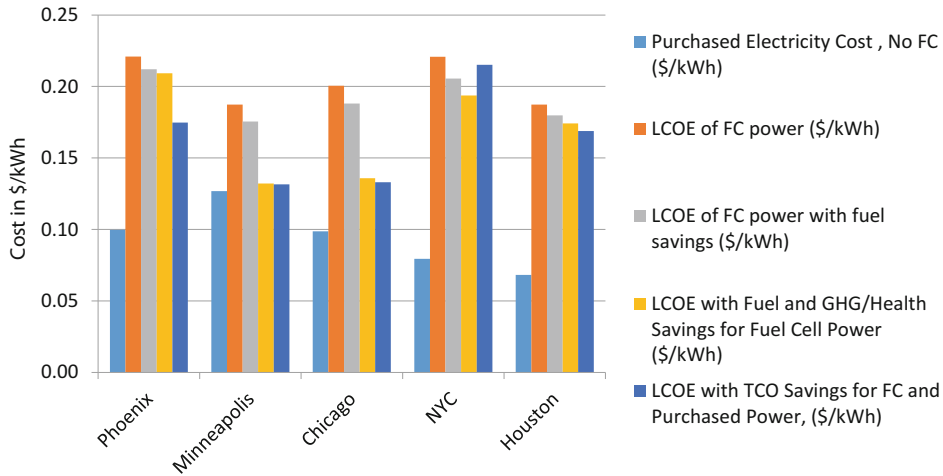
The cash flow for the case of a changing electricity grid with lower emissions due to the Clean Power Plan and other regulations is shown in Fig. 21c. In this case the TCO savings from a



Fuel Cell Systems: Total Cost of Ownership, Fig. 19 2015 costs of electricity for a 50 kW PEM CHP system in a small hotel. The fuel cell system’s LCOE with TCO savings is favorable in Minneapolis and Chicago

Fuel Cell Systems: Total Cost of Ownership, Table 17 LCC and LCIA output results for a 50 kWe PEM CHP system in a small hotel in five cities, assuming \$4000/kWe installed cost

Output	Phoenix, AZ		Minneapolis, MN		Chicago, IL		NYC, NY		Houston, TX	
	No FCS	Fuel cell	No FCS	Fuel Cell	No FCS	Fuel cell	No FCS	Fuel cell	No FCS	Fuel cell
Total electricity demand (kWh/yr)	576,668	576,668	419,590	419,590	424,147	424,147	369,661	369,661	497,656	497,656
Total space heating demand (kWh/yr)	23,307		174,743		135,869		135,869		0	
Total water heating demand (kWh/yr)	76,954		127,112		118,971		116,075		83,071	
Annual generated power by FC (kWh)		382,253		345,368		345,791		314,930		362,313
Annual generated heat by FC (kWh)		565,468		501,840		502,765		454,903		532,839
FC fraction of electricity demand		66%		82%		82%		85%		73%
Capital cost (\$/yr)		19,268		19,268		19,268		19,268		19,268
O&M cost (\$/yr)		11,468		10,361		10,374		9448		10,869
Scheduled maintenance (\$/yr)		1000		1000		1000		1000		1000
Fuel cost for fuel cell (\$/yr)		42,227		27,285		30,998		31,885		29,421
Fuel cost for conv. heating (\$/yr)	3574	831	7780	4504	7450	3972	8351	4504	2185	0
Purchased electricity Energy cost (\$/yr)	47,305	15,360	45,374	6679	32,104	4889	8798	6926	15,427	9524
Demand charge (\$/yr)	5445	3635	3422	1937	6021	3460	16,959	8882	15,490	9422
Fixed charge, electricity (\$/yr)	150	150	131	131	348	348	1241	1241	295	295
Total electricity cost (\$/yr)	52,899	93,108	48,927	66,662	38,473	70,337	26,998	78,650	31,213	79,800
Total cost of electricity (\$/kWh)	0.092	0.161	0.117	0.159	0.091	0.166	0.073	0.213	0.063	0.160
Purchased electricity cost (\$/kWh)	0.092	0.098	0.117	0.118	0.091	0.111	0.07303	0.311	0.063	0.142
LCOE of FC power (\$/kWh)		0.193		0.168		0.178		0.196		0.167
LCOE of FC power with fuel savings (\$/kWh)		0.186		0.158		0.168		0.183		0.161
LCOE with TCO savings for fuel cell power (\$/kWh)		0.178		0.065		0.057		0.172		0.146
LCOE with TCO savings for FC and purchased power, (\$/kWh)		0.151		0.074		0.067		0.193		0.145



Fuel Cell Systems: Total Cost of Ownership, Fig. 20 2030 costs of electricity for a 50 kW PEM CHP system in a small hotel with assumed reductions in

electricity grid emissions from the Clean Power Plan. The fuel cell system's LCOE with TCO savings is not favorable in any of the five cities

fuel cell (assuming static emission factors from the FCS) are seen to drop from about \$30,000 per year to about \$5000 per year. In this case the cash flow curve bends downward over time, and the societal cash flow is still net cash positive after 15 years, but the net cash flow in 2030 is reduced by about 80% from the static grid case above.

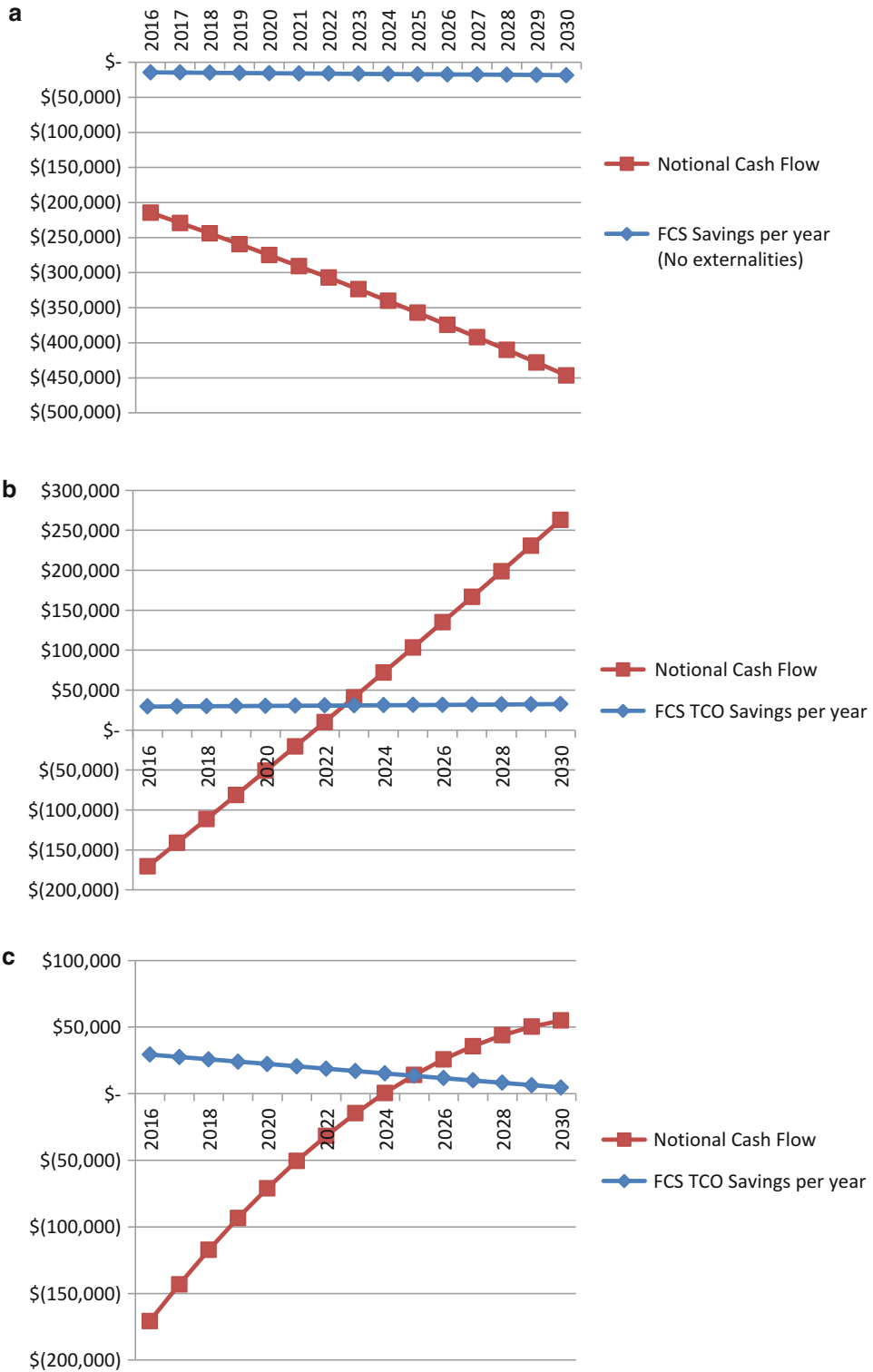
SOFC Fuel Cell System Manufacturing Costs

A typical SOFC stack is made up of two electrodes (anode and cathode), an electrolyte, seals, interconnect plates, and a frame (Fig. 22). The electrodes and electrolyte form the electrolyte-electrode assembly (EEA) and forms the core component of the fuel cell stack where the electrochemical reactions take place. An anode supporting layer and cathode supporting layer is often added to the EEA, which are designed to support the cathode and anode layers as shown in Fig. 23. This entry is primarily based on FCE/VersaPower's anode-supported cell architecture and reported process steps and stack materials. In an anode-supported cell, the anode layer provides the structural support for the electrically active components.

For an SOFC stack, the electrolyte is typically made up of a ceramic material such as yttria-

stabilized zirconia (YSZ) due to its good ionic conductivity and robust mechanical properties under high-temperature operation. The anode is made up of a porous cermet material composed of nickel mixed with YSZ to allow the fuel to be diffused to the reaction sites close to the electrolyte layer, for the oxygen ions to oxidize the fuel and for the delivered electrons to be conducted to the next cell or to the external load. The composition and manufacturing process for the EEA is summarized in Table 18. The seals prevent the mixing of fuel and oxidant within the stack, leaking of fuel and oxidant from the stack, as well as to provide mechanical bonding for the components [41]. Barium-calcium-aluminosilicate (BCAS), an alkaline earth aluminosilicate glass, is most commonly used for SOFC seals due to its high electrical resistivity, high thermal expansion, and rapid crystallization kinetics [42] and was modeled in this study.

The interconnections provide both electrical contacts and gas channels between individual cells. For SOFC systems, interconnects are usually made from metal material since they need to withstand temperatures up to 1000 °C and usually have a lower manufacturing cost than ceramic-based interconnects. The EEA, seals, and interconnects together form the "stack repeating unit"



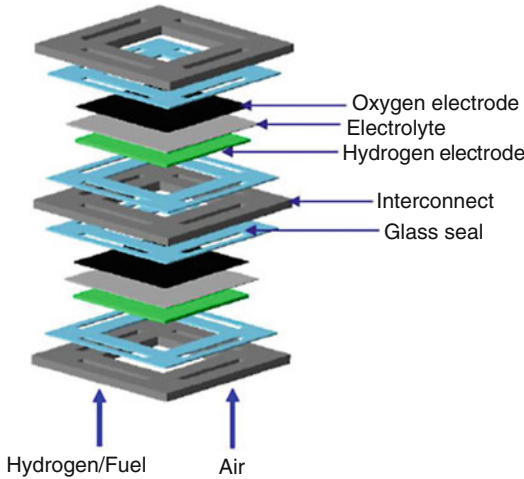
Fuel Cell Systems: Total Cost of Ownership, Fig. 21 Cash flows for a 50 kW PEM CHP system at \$r000/kWe installed cost for a small hotel in Chicago. (a)

Private cash flow and (b) societal cash flow with private and social costs with a static grid and (c) social cost with a cleaner grid under the Clean Power Plan

(SRU) of the cell. These repeating units are connected together to provide a wide range of power output, forming a “stack.” Finally, a support structure, such as endplates with tie rods, holds the fuel cell stack together to provide structural support. In this study, a base design with SS441 interconnect and frame is assumed where

the interconnect has a thickness of 630 630 μm and a mass of 247 grams [43].

Total fuel cell plate area is taken to be 540 cm². Active catalyzed area is about 61% of this area due to plate border regions and manifold openings. Single-cell active area has an additional 10% area loss due to the frame sealing process. The 10 kWe system consists of 130 cells in a single stack, while the 50 kW system has 5 stacks of 130 cells each. Only bottom-up costing details are presented in this section for the EEA assembly as an example and since this makes up the largest cost component of the SOFC stack. More details can be found in Scatagliini et al. [3].



Fuel Cell Systems: Total Cost of Ownership, Fig. 22 Typical SOFC stack configuration [18]

SOFC Stack Manufacturing Process Flow

Three different process parameters have been taken into account in the cost model: (i) “availability,” or the percentage of time that equipment is available to run during the total possible planned production uptime; (ii) “performance,” a measure of how well the equipment runs within its time of operation; and (iii) “process yield or quality,” a measure of the number of parts that meet specification compared to how many were produced.

A major challenge for fuel cell manufacturing cost modeling is that these parameters are not available since data collected by fuel cell manufacturers are not accessible, and each fuel cell manufacturer uses different toolsets, different manufacturing techniques, and produces no more than 100 MW per year. As in other costing studies [44–46], the model assumes that losses decrease with increasing manufacturing volumes and level of automation due to (i) improvement of in-line inspection with greater inspection sensitivity and more accurate response to defects and

Cathode Functional Layer (50 μm)
Cathode/Electrolyte Interlayer (10 μm)
Electrolyte Layer (10 μm)
Anode/Electrolyte Interlayer (10 μm)
Anode Functional Layer (700 μm)

Fuel Cell Systems: Total Cost of Ownership, Fig. 23 EEA schematic

Fuel Cell Systems: Total Cost of Ownership, Table 18 EEA composition and manufacturing process

Component	Materials	Thickness/μm	Process
Anode	Ni/YSZ	700	Tape casting
Anode electrolyte interlayer	50% YSZ 50% NiO	10	Screen printing
Electrolyte	YSZ (yttria-stabilized zirconia)	10	Screen printing
Electrolyte/cathode interlayer	50% YSZ 50% LSM	10	Screen printing
Cathode	LSM (lanthanum strontium manganite)	50	Screen printing

in-line signals, (ii) development of models that relate in-line metrics and measurements to output responses and performance [33], and (iii) utilization of greater feedback systems in manufacturing processing for real-time adjustment of process parameters.

Since vendors and industry advisors do not provide exact information about these parameters, the approach is to assume a range for each parameter as described below and then estimate intermediate values through exponential interpolation depending on annual production volume (Table 19). The advantage of introducing these parameters in the model is because, using sensitivity analysis, it is possible to estimate the impact of these parameters on manufacturing costs.

Line availability is assumed to be 80% and process yield to be 85% at low volumes (<100,000 EEA cells year⁻¹, 10 MWe). At the highest volumes (>10,000,000 EEA cells year⁻¹, 500 MWe year⁻¹), line availability and process yield are assumed equal to 95%. For volumes between 100,000 and 10,000,000 EEA cells year⁻¹, the process parameters are found through exponential interpolation. Line performance is considered equal to 89% for manual configuration and 95% for semiautomatic and automatic configurations. As a comparison, Fuel Cell Energy Inc. has reported a fabrication yield of 95% at a production volume of 500 kWe per year⁻¹ [43].

SOFC Stack Material Cost

Material costs are obtained from multiple vendors from Japan, the USA, and China. These countries are the primary suppliers for SOFC materials worldwide. Material prices are priced based on delivery to the geographical center of the USA. Material quality and prices from Chinese suppliers are also evaluated versus US distributors to determine their competitiveness.

Material prices for the EEA used in this study are shown in Table 20. For the EEA, material cost of each layer was calculated using the weight of the slurry constituents multiplied by the corresponding material cost (\$ kg⁻¹). For the anode-supported cell design, the anode materials contribute to about 75–82% of the EEA material

cost due to the thickness of the anode layer. Table 21 shows the material prices for the binders, plasticizers, pore formers, and solvents at different order quantities. As shown in the tables, material costs are highly dependent on annual production volume, especially for ceramic materials used in the fabrication of the EEA cells.

At high volumes, material cost is one of the dominant cost drivers in a SOFC stack. In most cases, material prices from Chinese suppliers are competitive with US-based suppliers, while prices from Japanese suppliers were the highest among all vendors.

Electrode-Electrolyte Assembly (EEA) Functional Cell

Based on a literature search and discussions with industry experts, the steps required for the fabrication of the EEA functional cell are:

1. Preparing the anode slurry using a two-step ball milling process
2. Sieving and de-airing of the anode slurry
3. Tape casting and infrared drying of the anode tape

Fuel Cell Systems: Total Cost of Ownership, Table 19 EEA manufacturing line process parameters for all annual production volumes

Power	Systems/year	Process yield (%)	Availability (%)	Line performance (%)
10	100	88%	80%	89%
	1000	91%	81%	95%
	10,000	92%	88%	95%
	50,000	93%	93%	95%
50	100	90%	80%	89%
	1000	92%	86%	95%
	10,000	93%	93%	95%
	50,000	94%	95%	95%
100	100	91%	81%	95%
	1000	92%	88%	95%
	10,000	94%	95%	95%
	50,000	95%	95%	95%
250	100	91%	84%	95%
	1000	93%	910%	95%
	10,000	94%	95%	95%
	50,000	95%	95%	95%

Fuel Cell Systems: Total Cost of Ownership, Table 20 Anode-supported cell material prices

Vendor/country	Material	Order quantity/kg	Price/\$ kg ⁻¹	Comments
Daiichi JITSUGYO (Japan)	Nickel oxide	1000	68.5	CIF USA by sea
		5000	42.5	CIF USA by sea
		10,000	37	CIF USA by sea
		20,000	34	CIF USA by sea
Daiichi JITSUGYO (Japan)	8YSZ (8 mol%YSZ)	100	78	CIF USA by sea
		1000	68	CIF USA by sea
		5000	63	CIF USA by sea
Daiichi (Japan)	8YSZ (8 mol%YSZ)	10	97	CIF USA by sea
		100	95	CIF USA by air
		1000	83	CIF USA by sea
Inframat Advanced Materials (USA)	8YSZ (8 mol%YSZ)	1	139.2	By rail or truck
		5	115.8	By rail or truck
		10	94.5	By rail or truck
		50	71.6	By rail or truck
		100	49.7	By rail or truck
		1000	35.2	By rail or truck
		10,000	29.8	By rail or truck
Inframat Advanced Materials (USA)	LSM powder	100	170	By rail or truck
		1000	95	By rail or truck
		10,000	70	By rail or truck
Qingdao Terio Corporation (China)	LSM powder	10	250	CIF USA by air
		100	150	CIF USA by air
		200	125	CIF USA by air
		500	105	CIF USA by air
		1000	80	CIF USA by air
		2000	75	CIF USA by air
5000	60	CIF USA by air		

CIF price including cost, insurance, and freight

4. Rolling in a take-up roll of the green tape
5. Cutting and blanking into sheets of the green tape
6. Screen printing and infrared drying of subsequent layers (anode-electrolyte interlayer, electrolyte, cathode-electrolyte interlayer, and cathode layer) above the anode sheet
7. First quality check (infrared imaging and ultrasonic spectroscopy)
8. Bonding together the mini-stack of five layers by placing it in a furnace at elevated temperature (~1300–1400 °C) for 24 h [47, 48]
9. Laser cutting of the EEA cell to the proper dimensions;
10. Final quality check (infrared imaging, ultrasonic spectroscopy, and vacuum leak test)

In this entry, slurries are prepared by a two-step ball milling process. In the first step, solid powders are ball milled for 12 h in solvent. In the second step, binder and plasticizer are added and then ball milled for another 12 h [49]. Quantities of slurry to mill per day are estimated based on number of cells casted per day and slurry weight of each layer. Slurry drying time is estimated using the average evaporation rate value of aqueous slurry described by Mistler et al. [50] as suggested in a Battelle report [51]. Assuming that the ratio of the freshly deposited layer thickness to the dried tape thickness is two [52] and multiplying this freshly deposited layer thickness by its corresponding liquid density, it was possible to obtain the quantity of liquid removed per unit area. The corresponding slurry drying time

Fuel Cell Systems: Total Cost of Ownership, Table 21 Binders, plasticizers, pore formers, and solvent prices

Vendor/country	Material	Order quantity/kg	Price/\$ kg ⁻¹	Comments
Jiangsu Xiangcanghongrun Trade Co., Ltd. (China)	N-butyl acetate 99,5%	100	4.34	CIF USA by sea
		1000	1.516	CIF USA by sea
		10,000	1.29	CIF USA by sea
ChemPoint Inc. (USA)	Methocel A4M	1–45,400	18.5–29.6	CIF price
Dowd & Guild, Inc. (CA)	Butvar B-76	63.5	23.37	By rail or truck
		200	21.42	By rail or truck
		500	19.47	By rail or truck
		1000	18.36	By rail or truck
		2000	17.14	By rail or truck
		5000	16.07	By rail or truck
Univar (USA)	Santicizer 160	Confidential information from vendor		
Cancarb Limited (USA)	Thermax [®] N990 thermal carbon black	Confidential information from vendor		
Jinan Shijitongda Chemical Co., Ltd. (China)	2-Butoxyethanol	1000	3.07	CIF USA
		10,000	3.07	CIF USA
		100,000	2.53	CIF USA
		1000,000	2.32	CIF USA
		10,000,000	2.29	CIF USA

CIF price including cost, insurance, and freight

is estimated dividing the quantity of liquid removed per unit area by an average evaporation rate of the solvent equal to 2.22×10^{-5} g cm⁻² s⁻¹ at room temperature for an air flow rate of 75 l min⁻¹ [51]. Estimated slurry drying times are 24.7 min for the anode slurry, 0.48 min for the electrolyte slurry, 2.2 min for the cathode slurry, and 0.44 min for interlayer slurries. In reality, evaporation rates may be expected to be faster than the ones considered in this study since water evaporates more slowly than most organic solvents as n-butyl acetate or 2-butoxyethanol [53].

Equipment size, cycle times, and level of automation vary with annual production rates. Tape casting machines are sized depending on production volume, slurry drying time, and casting speed. Tape casting speed varies with annual production volume

and machine size from 0.25 to 1 m min⁻¹. Subsequent process modules included in the production line are sized based on the estimated production capacity and cycle time of the tape casting machine.

SOFC Stack Direct Manufacturing Costs

Table 22 shows the cost model results for all system sizes and production rates. Considering the base design, stack cost per unit of electrical power (\$ kWe⁻¹) decreases both with increasing system size and increasing annual production rate. When comparing the two key cost drivers, cost seems to be somewhat more sensitive to system size than to production rate, and the impact of system size diminishes at higher production volumes.

Fuel Cell Systems: Total Cost of Ownership, Table 22 SOFC stack costs [3]

System size (kW)	100 systems/yr	1000 systems/yr	10,000 systems/yr	50,000 systems/yr
10	1039	342	197	178
50	478	215	176	170
100	339	194	171	168
250	249	181	167	166

Figure 24 shows stack manufacturing costs broken out by component for 10 kWe systems. The largest contributor to the stack manufacturing cost is the EEA, which constitutes about 50% of total cost in all cases analyzed. Interconnect and cell-to-frame seal each constitute 11–15% of the stack cost and decrease with production volume. Stack assembly and conditioning process remains constant at about 9% of the stack cost. The relative contribution of frame manufacturing cost to overall stack cost increases with production volume since at low volumes, it is assumed that interconnect manufacturing lines are used and there is no capital cost and building cost associated with the frames.

At low volumes, process capital and labor costs are the categories that most affect the stack cost, whereas at high volume, material cost dominates followed by process capital cost. Figure 25 demonstrates that with increasing production, volume process/operational costs increase and labor cost decreases at greater level of automation. Capital and building costs decrease due to the higher equipment utilization, and scrap cost decreases since the cost model assumes lower defective rate at higher production volumes.

SOFC Balance of Plant and System Costs

The balance of plant analysis approach is similar to that for PEM FCS described above (Table 23). Since the SOFC is a higher-temperature process than PEM, the overall balance of plant is simpler in terms of requiring fewer components and has overall lower cost. For example, the SOFC unit in Fig. 9 has a smaller reformer unit, no post-reformer cleanup, and no air humidification system. Again the BOP is subdivided into six subsystems:

1. Fuel subsystem
2. Air subsystem

3. Heat management subsystem
4. Power subsystem
5. Control and meter subsystem
6. Miscellaneous subsystem

Overall the BOP cost for SOFC systems is estimated to be about 35% lower per kWe than PEM at annual production rates of greater than about 10 MW.

For the CHP reformat system, the power subsystem represents the largest subsystem cost for the 100 kWe system, representing approximately 40% of the total BOP, following by the control and meter subsystem. In particular, the power inverter is a dominant cost driver, representing approximately 80% of the cost in the power subsystem (Table 15).

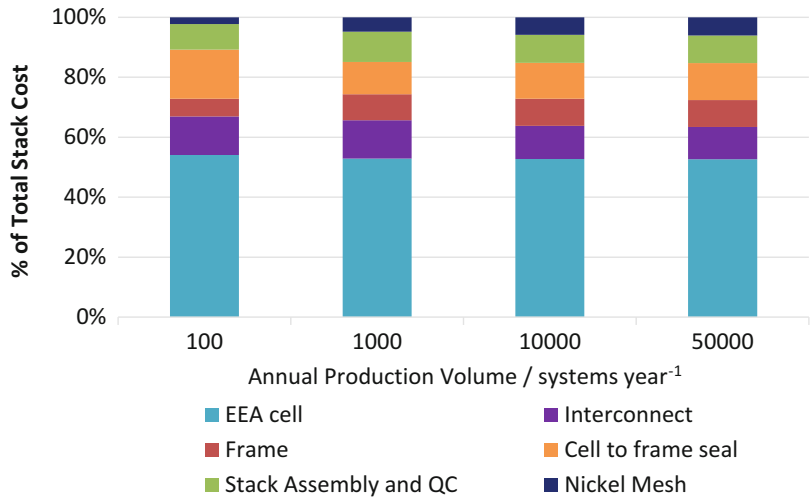
Direct system costs for CHP are shown in Fig. 26. For a 50 kWe system at 100 units per year, a customer cost of \$3000/kWe for an installed system is assumed, or about double the direct system cost assuming similar corporate markup and installation costs as for the PEM case above.

SOFC vs. PEM Fuel Cell CHP Balance of Plant and System Costs

A summary of fuel cell stack, balance of plant, and direct system costs for SOFC and PEM fuel cell CHP systems is shown in Table 24. Focusing on the 50 kWe system size, the stack cost is estimated to be lower for SOFC by about 20–30% across manufacturing values, the BOP is between 30% and 40% lower, and the overall direct cost is about 25–35% lower. For both PEM and SOFC, the BOP is the dominant component of cost at about 70–80% of direct system cost with the BOP share of cost increasing as annual volume increase.

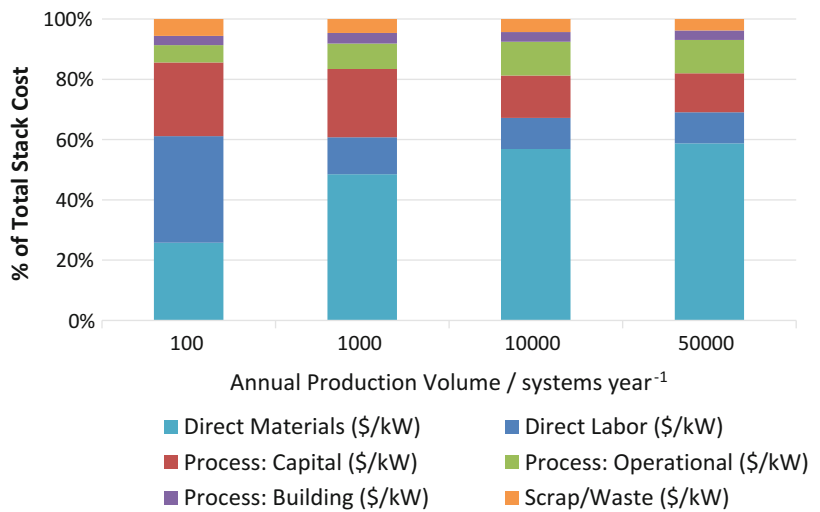
Fuel Cell Systems: Total Cost of Ownership,

Fig. 24 Disaggregation of stack cost by relative percentage of stack components cost to overall stack cost for 50 kWe systems [3]



Fuel Cell Systems: Total Cost of Ownership,

Fig. 25 Disaggregation of stack cost by relative percentage of cost components to overall stack cost for 50 kWe systems [3]



Fuel Cell Systems: Total Cost of Ownership, Table 23 Summary of BOP costs in \$/kWe for SOFC CHP [3]

System size	100 units/year	1000 units/year	10,000 units/year	50,000 units/year
250 kWe	\$ 693	\$ 488	\$ 419	\$ 365
100 kWe	\$ 807	\$ 564	\$ 479	\$ 422
50 kWe	\$ 1002	\$ 721	\$ 611	\$ 537
10 kWe	\$ 1638	\$ 1217	\$ 1027	\$ 925

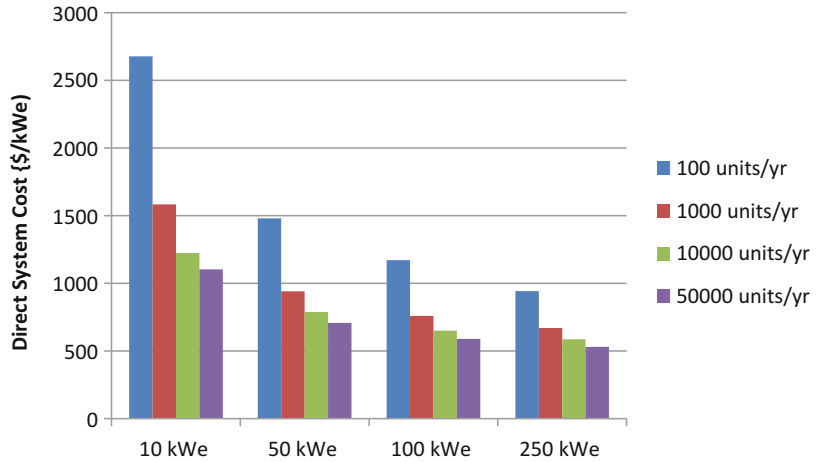
SOFC CHP System Life-Cycle Cost and LCIA Model Example

Example output of the LCC/LCIA model for a 50 kW small hotel in five representative cities is shown in Table 25. The cost of electricity in 2015 is shown in Fig. 27 for the case of a 50 kW SOFC fuel cell system in a small hotel at an installed cost of

\$3000/kWe. As in the PEM FC technology case above, the first bar is the reference cost of electricity for the reference case of no fuel cell system in a 50 kW small hotel and the second bar is the LCOE from the fuel cell system. The third and fourth bars are the reduction in FC LCOE with heating fuel savings and then with health and environmental

Fuel Cell Systems: Total Cost of Ownership,

Fig. 26 Direct costs for SOFC CHP systems as a function of system size and manufacturing volume [3]



savings, respectively. The final bar is the LCOE with TCO savings for the fuel cell system case with electricity from the fuel cell system and with any purchased electricity from the grid. There is a net reduction in electricity cost in Minneapolis and Chicago which is driven by the health and environmental externality savings.

The estimated cost of electricity in 2030 is shown in Fig. 28 with the same sequence of costs as above assuming a cleaner electricity grid under the Clean Power Plan. In this case, the LCOE with TCO savings for FC and purchased power is still lower than the cost of electricity in the reference case without a fuel cell system in Minneapolis and Chicago.

Figure 29a, b shows the private cash flow and societal cash flow in the case of a static electricity grid. As with the PEM system, the private cash flow is negative, but TCO savings in the latter case generates positive cash flow after about 2 years. Even with the Clean Power Plan and a lower polluting electricity grid, the societal cash flow is strongly net positive in 2030 (Fig. 29c).

Summary

Discussion

All fuel cell stack components (CCM, GDL, framed MEA, plates and stack assembly for PEM and EEA, plate, frame, and stack assembly for SOFC) are assumed to be manufactured in-house with high throughput processes and

high yield ($\geq 95\%$) assumed for all modules at high manufacturing volumes. Direct cost results for the stack will be highly dependent on the yield assumptions for each process module. Here, nearly fully automated roll-to-roll processing is modeled for the critical catalyst-coated membrane and for the GDL.

The assumed yield rates are a key uncertain variable in estimating fuel cell stack manufacturing costs. While it was not in the scope of this entry to do a detailed yield feasibility analysis, well-established methodologies exist for improving yield using similar process modules in other industries, and learning by doing and improvements in yield inspection, detection, and process control are implicitly assumed. This entry assumes that high yield is achieved at high manufacturing volumes. This stems from several implicit assumptions.

Learning by doing over the cumulative volume of fuel cell component production and greater process optimization will drive yield improvement both within a given vendor and from vendor to vendor through industry interactions (conferences, IP, cross vendor personnel transfers, etc.):

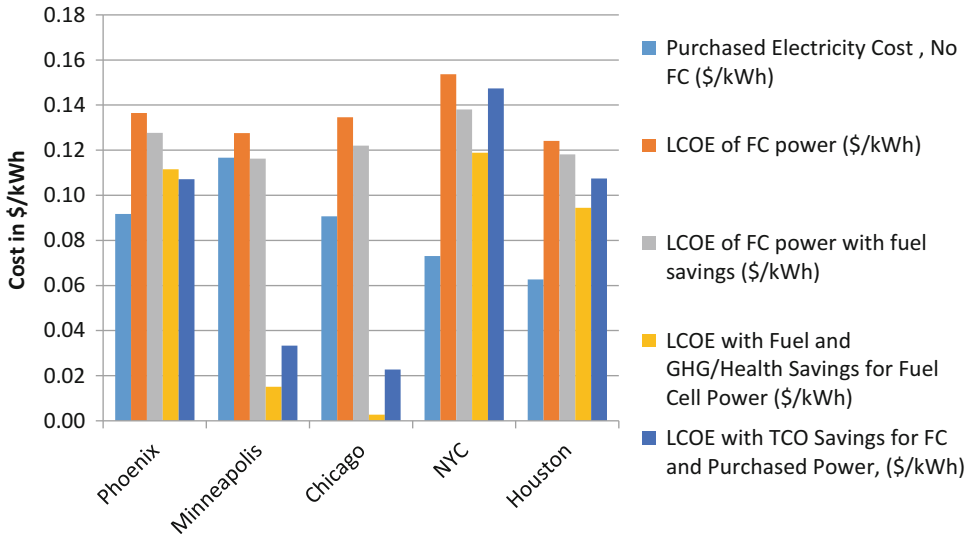
- In-line inspection improvement with greater inspection sensitivity and more accurate response to defects and in-line signals.
- Greater development and utilization of “transfer functions” (Manhattan Projection [33]), e.g., development of models that relate in-line

Fuel Cell Systems: Total Cost of Ownership, Table 24 Direct costs for PEM and SOFC CHP fuel cell systems as a function of system size and annual manufacturing volume

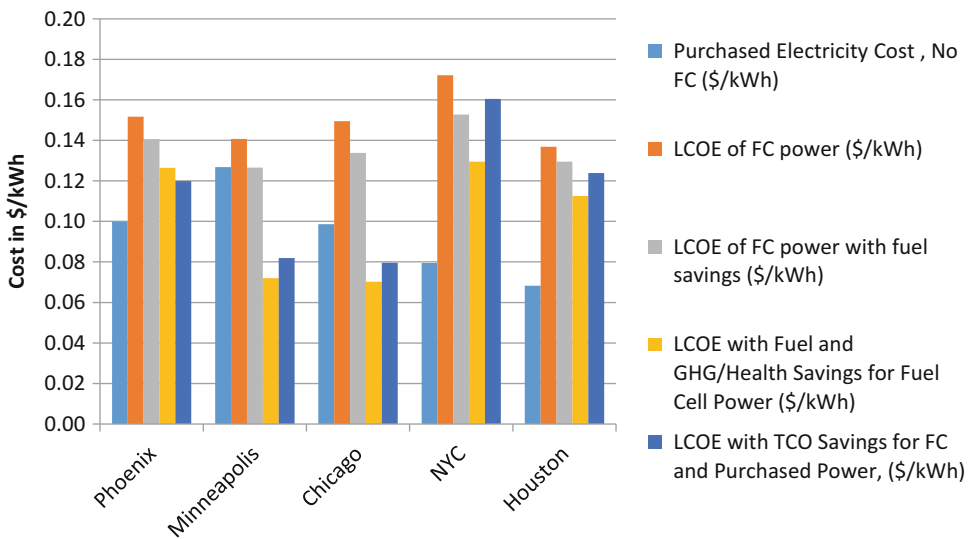
System size {kW}	Fuel cell stack (PEM)				Fuel cell stack (SOFC)				SOFC cost reduction (stack)			
	100 units/year-1	1000 units/year-1	10,000 units/year-1	50,000 units/year-1	100 units/year-1	1000 units/year-1	10,000 units/year-1	50,000 units/year-1	100 units/year-1	1000 units/year-1	10,000 units/year-1	50,000 units/year-1
10 kWe	340	497	333	284	1039	342	197	178	22%	31%	41%	37%
50 kWe	596	352	272	239	478	215	176	170	20%	39%	35%	29%
100 kWe	466	313	249	219	339	194	171	168	27%	38%	31%	23%
250 kWe	377	279	231	203	249	181	167	166	34%	35%	28%	18%
	Balance of plant (PEM)				Balance of plant (SOFC)				SOFC cost reduction (BOP)			
System size {kW}	100 units/year-1	1000 units/year-1	10,000 units/year-1	50,000 units/year-1	100 units/year-1	1000 units/year-1	10,000 units/year-1	50,000 units/year-1	100 units/year-1	1000 units/year-1	10,000 units/year-1	50,000 units/year-1
10 kWe	2703	2177	1792	1612	1638	1217	1027	925	39%	44%	43%	43%
50 kWe	1439	1188	982	881	1002	721	611	537	30%	39%	38%	39%
100 kWe	1097	894	744	676	807	564	479	422	26%	37%	36%	38%
250 kWe	852	719	622	562	693	488	419	365	19%	32%	33%	35%
	System direct cost (PEM)				System direct cost (SOFC)				SOFC cost reduction (SYSTEM)			
System size {kW}	100 units/year-1	1000 units/year-1	10,000 units/year-1	50,000 units/year-1	100 units/year-1	1000 units/year-1	10,000 units/year-1	50,000 units/year-1	100 units/year-1	1000 units/year-1	10,000 units/year-1	50,000 units/year-1
10 kWe	4043	2674	2125	1896	2677	1559	1224	1103	34%	42%	42%	42%
50 kWe	2035	1540	1254	1120	1480	936	787	707	27%	39%	37%	37%
100 kWe	1563	1207	993	895	1146	758	650	590	27%	37%	35%	34%
250 kWe	1229	998	853	765	942	669	586	531	23%	33%	31%	31%
	BOP share of total cost (PEM)				BOP share of total cost (SOFC)							
System size {kW}	100 units/year-1	1000 units/year-1	10,000 units/year-1	50,000 units/year-1	100 units/year-1	1000 units/year-1	10,000 units/year-1	50,000 units/year-1				
10 kWe	67%	81%	84%	85%	61%	78%	84%	84%				
50 kWe	71%	77%	78%	79%	68%	77%	78%	76%				
100 kWe	70%	74%	75%	76%	70%	74%	74%	72%				
250 kWe	69%	72%	73%	73%	74%	73%	72%	69%				

Fuel Cell Systems: Total Cost of Ownership, Table 25 LCC and LCIA output results for a 50 kWe SOFC CHP system in a small hotel in five cities, assuming \$3000/kWe installed system cost

Output	Phoenix, AZ		Minneapolis, MN		Chicago, IL		NYC, NY		Houston, TX	
	No FCS	Fuel cell	No FCS	Fuel cell	No FCS	Fuel cell	No FCS	Fuel cell	No FCS	Fuel cell
Total electricity demand (kWh/yr)	576,668	576,668	419,590	419,590	424,147	424,147	369,661	369,661	497,656	497,656
Total space heating demand (kWh/yr)	23,307		174,743		135,869		135,869		0	
Total water heating demand (kWh/yr)	76,954		127,112		118,971		116,075		83,071	
Annual generated power by FC (kWh)		382,253		345,368		345,791		314,930		362,313
Annual generated heat by FC (kWh)		90,829		145,416		142,764		142,049		78,340
FC fraction of electricity demand		66%		82%		82%		85%		73%
Capital cost (\$/yr)		14,451		14,451		14,451		14,451		14,451
O&M cost (\$/yr)		11,468		10,361		10,374		9448		10,869
Scheduled maintenance (\$/yr)		1000		1000		1000		1000		1000
Fuel cost for fuel cell (\$/yr)		25,252		18,254		20,705		23,481		18,629
Fuel cost for conv. heating (\$/yr)	3574	201	7780	3875	7450	3102	8351	3447	2185	39
Purchased electricity energy cost (\$/yr)	47,305	15,360	45,374	6679	32,104	4889	8798	6926	15,427	9524
Demand charge (\$/yr)	5445	3635	3422	1937	6021	3460	16,959	8882	15,490	9422
Fixed charge, electricity (\$/yr)	150	150	131	131	348	348	1241	1241	295	295
Total electricity cost (\$/yr)	52,899	71,316	48,927	52,813	38,473	55,227	26,998	65,428	31,213	64,191
Total cost of electricity (\$/kWh)	0.092	0.124	0.117	0.126	0.091	0.130	0.073	0.177	0.063	0.129
Purchased electricity cost (\$/kWh)	0.092	0.098	0.117	0.118	0.091	0.111	0.07303	0.311	0.063	0.142
LCOE of FC power (\$/kWh)		0.136		0.128		0.135		0.154		0.124
LCOE of FC power with fuel savings (\$/kWh)		0.128		0.116		0.122		0.138		0.118
LCOE with TCO savings for fuel cell power (\$/kWh)		0.111		0.015		0.003		0.119		0.094
LCOE with TCO savings for FC and purchased power (\$/kWh)		0.107		0.033		0.023		0.147		0.107



Fuel Cell Systems: Total Cost of Ownership, Fig. 27 2015 costs of electricity for a 50 kW SOFC CHP system in a small hotel. The fuel cell system’s LCOE with TCO savings is favorable in Minneapolis and Chicago

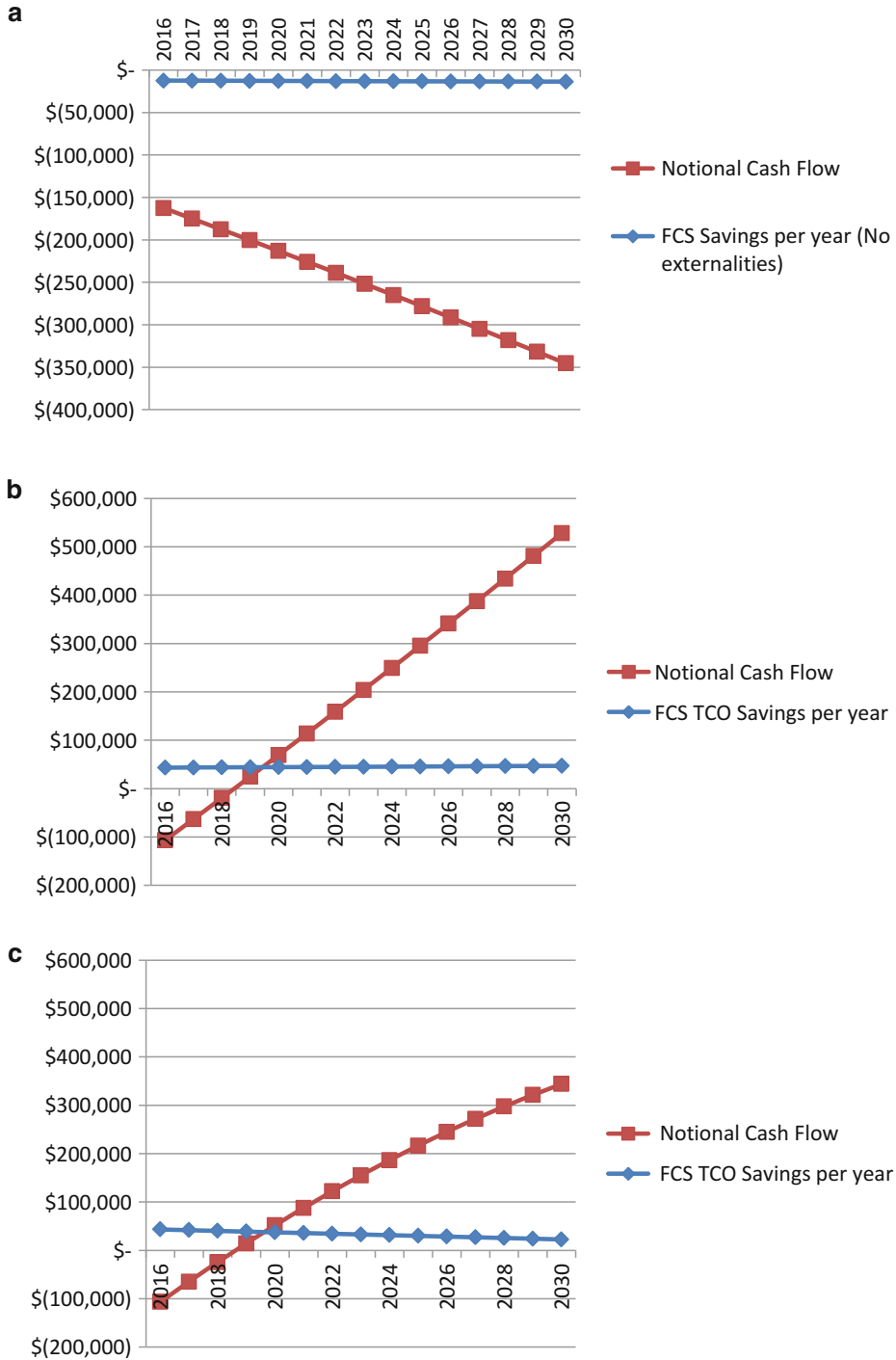


Fuel Cell Systems: Total Cost of Ownership, Fig. 28 2030 costs of electricity for a 50 kW SOFC CHP system in a small hotel with assumed reductions in

electricity grid emissions from the Clean Power Plan. The fuel cell system’s LCOE with TCO savings is still favorable in Minneapolis and Chicago

- metrics and measurements to output responses and performance, and resultant improvement in in-line response sensitivity and process control.
- Utilization of greater feedback systems in manufacturing processing such as feed-forward sampling, for real-time adjustment of

- process parameters (e.g., slot die coating thickness and process parameter control).
- Systematic, integrated analysis to anticipate and prepare for yield excursions, e.g., FMEA (failure modes and effect analysis).
- Consideration of yield limiting mechanisms or FMEA-type analysis as a function of



Fuel Cell Systems: Total Cost of Ownership, Fig. 29 Cash flows for a 50 kW SOFC CHP system at \$3000/kWe installed cost for a small hotel in Chicago. (a)

Private cash flow and (b) societal cash flow with private and social costs with a static grid and (c) social cost with a cleaner grid under the Clean Power Plan

process tooling assumptions is out of scope here and would be very challenging in this type of analysis entry without access to manufacturing data.

At low volumes, PEM stack cost is sharply reduced when moving from a production volume of 100 to 1000 systems per year since tool utilization increases rapidly and capital costs drop sharply. At high volumes, the stack cost is seen to fall at a rate between 20% and 30% per decade increase in volume. This is driven by improved yield and lower direct material costs (e.g., membrane and carbon fiber paper).

Direct material costs dominate PEM stack costs at high volume. For fuel cell stacks in CHP systems with reformat fuel at high production volumes, CCM manufacturing is about 55% of manufacturing cost, with plates at about 20%, and frame and seal about 15%. In terms of cost dominating factor, it was found that yield, power density, and Pt price are the most contributing factors to the overall stack cost.

For SOFC stacks, the EEA makes up about 50% of the stack cost at all annual production volumes, followed by the cell-sealing process at 10–18%, and interconnects at 10–15% of the stack manufacturing cost. The process yield and power density are the most sensitive parameters for the stack cost at both low and high annual production volumes. At low production volumes (5MWe per year), line performance and labor rate are the next most sensitive parameters, while at high production volume (2500 MWe per year), material costs and tool availability also become important cost sensitivities.

Under the assumptions of this entry, SOFC stack and system cost are significantly lower than PEM FCS. A representative 50 kWe system SOFC stack costs us 20–30% lower than PEM, BOP costs are 30–40% lower, and overall direct manufacturing cost is 25–35% than PEM. The SOFC stack does not require a precious metal catalyst, and the SOFC balance of plant has a lower number of components because of higher-temperature operation, and these factors lead to overall lower manufacturing cost.

This entry did not consider detailed DFMA-type cost analysis for balance of plant components. The case of BOP components built in-house was not considered (i.e., “make” versus “buy”) because many BOP components are commodity parts (e.g., pumps, compressors, tanks, motors, cabinets, variable frequency drives, tubing, piping, inverters, valves, heat exchangers, switches, flow sensors) for especially the larger CHP systems. Hence, this assumes that it would be less expensive to purchase these commodity components rather than manufacturing them in-house. Fuel cell manufacturers are unlikely to embark upon a program of producing BOP commodity parts in-house, with some exceptions still being investigated. Thus, the BOP is largely assumed to be comprised of purchased components that are either assembled or integrated by a fuel cell system manufacturer. The downside of this approach is that a fuel cell system provider may be forced to make nonoptimal design choices based on the availability of component part sizes. In some cases, customized design of non-commodity parts is required, as in the case of a manifold block for lower-power systems, but in these cases, the part is assumed to be designed by the fuel cell system provider and purchased from a contract manufacturer. However, many of these components could be readily produced in larger volume in the future, e.g., machined aluminum blocks, and perhaps as more integrated subassemblies. BOP integration and cost reductions realized therein seem more critical at lower system sizes where BOP costs are expected to comprise a larger fraction of overall system costs. In such cases, a FC manufacturer might work closely with a contract manufacturer or part vendor to prototype and develop such subassemblies. This type of part integration and subassembly design was not explicitly considered in this entry, but may represent further cost-reduction opportunities. Similarly, a rigorous examination of in-house manufacturing vs. external purchase was not done for every part and may also yield cost saving opportunities for some balance of plant components or assemblies. Since BOP is estimated to be a large fraction of overall costs,

Fuel Cell Systems: Total Cost of Ownership, Table 26 US Department of Energy equipment cost targets for 2020 and estimated costs in this entry

System	Units/yr	2020 DOE target with markup (\$/kW)	PEM direct cost (\$/kW)	PEM cost with 50% markup (\$/kW)	SOFC direct cost (\$/kW)	SOFC cost with 50% markup (\$/kW)
		DOE targets	This work			
10 kW CHP system	50,000	\$1700	\$1896	\$2844	\$1103	\$1655
100 kW CHP system	1000	\$1000	\$1207	\$1810	\$758	\$1137

this general area of part integration and consolidation and design optimization is a critical area for future work.

Comparison to DOE 2020 Targets

The output of this entry can also be compared with DOE targets for 2020 (Table 26). For 10 kWe CHP systems at 50,000 units per year, the DOE target is \$1700/kWe, and for 100 kWe and 1000 units per year, the equipment cost target is \$1000/kWe. This entry estimates that PEM equipment cost (direct cost with an assumed 50% equipment markup is about 70–80% higher than the DOE targets, while the SOFC system is meeting the 10 kWe target and within 15% of the 100 kWe target.

Conclusions

Direct costs are estimated for PEM and SOFC FC CHP systems from 10 to 250 kWe sizes and for annual manufacturing volumes of 100 systems per year to 50,000 systems per year. Key assumptions include vertically integrated manufacturing and high speed, relatively high-yield stack deposition processes for the membrane electrode or electrode/electrolyte assembly, and cost reductions in material costs with higher-volume purchases from material suppliers. Implicit in these assumptions is the assumption of continuous “learning by doing” as manufacturing volumes increase to improve process yields and accumulation of knowledge regarding best manufacturing processes and defect mode characterization and understanding.

Bottom-up DFMA costing analysis for fuel cell stack components in this entry shows that, for

stationary applications, PEM fuel cell stacks alone can approach a direct manufacturing cost of \$200 per kWe of net electrical power at high production volumes (e.g., 250 kW CHP systems at 50,000 systems per year). Overall system costs including corporate markups and installation costs are estimated to reach \$2200/kWe (\$1600/kWe) for 50 kW (250 kW) CHP systems at 50,000 systems per year.

SOFC fuel cell stacks can approach a direct manufacturing cost of \$165 per kWe of net electrical power at high production volumes (e.g., 250 kWe CHP systems at 50,000 systems per year). Overall SOFC system costs including corporate markups and installation costs are estimated to reach \$1400/kWe and \$1100/kWe for 50 kW (250 kW) CHP systems at 50,000 systems per year.

For both PEM and SOFC, balance of plant costs including the fuel processor makes up about 70–80% of total direct costs for 50 kWe CHP systems across the range of production volumes and is thus a key opportunity for further cost reduction. In general, the BOP has a lower rate of decrease in cost as a function of volume as the fuel cell stack in part because many components are already manufactured in reasonable volume and do not benefit in the same way from increased economies of scale as the fuel cell stack. This result is also influenced by the different methodologies applied to stack vs. BOP costing: a DFMA analysis was applied to the stack, whereas BOP costs were estimated based on largely purchased components and vendor price quotes.

The cost of electricity with and without total cost of ownership TCO credits for a fuel cell CHP

system has been demonstrated for buildings in five US cities. This approach incorporates the impacts of offset heating demand by the FCS, carbon credits, and environmental and health externalities into a total levelized cost of electricity (\$/kWh). This “LCOE with total cost of ownership credits” can then be compared with the baseline cost of grid electricity. This entry combines a fuel cell system use-phase model with a life-cycle integrated assessment model of environmental and health externalities. Total cost of electricity is dependent on the carbon intensity of the electricity grid and heating fuel that a FC system is displacing and thus highly geography dependent.

For example, in commercial building types considered here (small hotels), overall TCO costs of fuel cell CHP systems at current low production volume (e.g., 50 kWe systems at 100 systems per year) relative to grid power exceed prevailing power rates in Phoenix, New York City, and Houston, but can be competitive in regions of the country with higher carbon intensity grid electricity. Including total cost of ownership credits can bring the levelized cost of electricity below the cost of electricity purchased from the grid in Minneapolis and Chicago for both PEM and SOFC CHP systems. Health and environmental externalities can provide large savings if electricity or heating with a high environmental impact is being displaced. These externality benefits from fuel cell CHP systems are expected to diminish as the electricity grid becomes cleaner, assuming that FCS systems continue to be fueled by natural gas. In the modeled scenario here, simulating the impact of the proposed Clean Power Plan, the levelized cost of electricity with TCO credits becomes higher than the cost of grid electricity in 2030 for Minneapolis and Chicago in the PEM case, but remains lower than the cost of grid electricity in 2030 for these two locations in the SOFC case.

Overall, this type of total cost of ownership analysis quantification is important to identify key opportunities for direct cost reduction, to fully value the costs and benefits of fuel cell

systems in stationary applications, and to provide a more comprehensive context for future potential policies.

Future Directions

Key uncertainties in this type of modeling are the exact “state-of-the-art” design details for PEM and SOFC stacks, the actual process yields of stack process modules, and the details of stack composition and materials. Reverse engineering of a commercial fuel cell through stack performance characterization and cross sectional analysis of an actual fuel cell stack would provide valuable information but is beyond the scope of this entry. Additional future work includes further detailed study of lower power (1–5 kWe) fuel cell stack design and manufacturing and expanding the scope of the analysis to include more detailed study of balance of plant costs (e.g., balance of plant designs, supply chains, and comparisons to analogous industries).

As noted above, for both PEM and SOFC, balance of plant costs including the fuel processor make up about 70–80% of total direct costs for 50 kWe CHP systems across the range of production volumes and are thus a key opportunity for further cost reduction.

Further work in TCO analysis and modeling should explore providing a greater degree of temporal resolution for the marginal emission factors for the electricity system and higher temporal and spatial resolution of marginal benefit of abatement factors from the electricity grid. As in this entry, future modeling should try to incorporate the dynamic nature of the electricity grid portfolio and projected fuel prices as well as incorporate future projected equipment prices or learning rates in estimating future FCS CHP benefits.

From a policy standpoint, the illustration here of TCO costs that have appreciable credits in certain regions of the country is an important result that suggests that regionally specific policies and incentives may be appropriate. A key policy question is how to monetize these externalities, for example, where to provide incentives along the supply chain and how best to design policies for various stakeholders.

Bibliography

Primary Literature

- Darrow K, Tidball R, Wang J, Hampson A (2015) Catalog of CHP technologies. U.S. EPA (Environmental Protection Agency) Combined heat and power partnership. https://www.epa.gov/sites/production/files/2015-07/documents/catalog_of_chp_technologies.pdf
- Wei M, Lipman T, Mayyas A, Chien J, Chan SH, Gosselin D, Breunig H, Stadler M, McKone T, Beattie P, Chong P, Colella WG, James BD (2014) A total cost of ownership model for low temperature PEM fuel cells in combined heat and power and backup power, LBNL-6772E. Lawrence Berkeley National Laboratory, Berkeley
- Scataglini R, Mayyas A, Wei M, Chan SH, Lipman T, Gosselin D, D'Alessio A, Breunig H, Colella WG, James BD (2015) A total cost of ownership model for solid oxide fuel cells in combined heat and power and power-only applications. Lawrence Berkeley Laboratory Report LBNL-1005725
- Colella WG (2003) Modelling results for the thermal management sub-system of a combined heat and power (CHP) fuel cell system (FCS). *J Power Sources* 118:129–149
- Ormerod RM (2003) Solid oxide fuel cells. *Chem Soc Rev* 32:17–28
- DOE (2014) – Multi-year research, development and demonstration plan. http://energy.gov/sites/prod/files/2014/12/f19/fcto_myrrdd_fuel_cells.pdf
- James BD, Kalinoski JA, Baum KN (2010) Mass production cost estimation for direct H₂ PEM fuel cell systems for automotive applications, 2010 Update. Directed Technologies, Arlington
- Sinha J (2010) Direct hydrogen PEMFC manufacturing cost estimation for automotive applications, 2010 DOE annual merit review, Washington, DC, 9 June 2010. Project ID # FC019
- Marcinkoski J, James BD, Kalinoski JA, Podolski W, Benjamin T, Kopasz J (2011) Manufacturing process assumptions used in fuel cell system cost analyses. *J Power Sources* 196(12):5282–5292. ISSN 0378-7753, <https://doi.org/10.1016/j.jpowsour.2011.02.035>
- Mahadevan, K, Contini V, Goshe M, Price J, Eubanks F, Griesemer F (2010) Economic analysis of stationary PEM fuel cell systems. In: 2010 annual merit review proceedings, Department of energy, hydrogen and fuel cells program, Washington, DC
- James BD, Spisak AB, Colella WG (2012) Manufacturing cost analysis of stationary fuel cell systems. Strategic Analysis, Inc, Arlington
- Krullam K, Iyengar A, Kearns D, Newby D (2013) Assessment of the distributed generation market potential for solid oxide fuel cells, DOE/NETL-342/093013
- Staffell I, Green R (2013) The cost of domestic fuel cell micro-CHP systems. *Intl J Hydrogen Energy* 38:1088–1102
- E4tech (2014) The fuel cell industry review 2014. Available at 727 <http://www.e4tech.com/fuelcellindustryreview/>. Accessed on 10 Dec 2015
- Wei M, Smith SJ, Sohn MD (2017) Experience curve development and cost reduction disaggregation for fuel cell markets in Japan and the US. *Appl Energy* 191(1):346–357. ISSN 0306-2619, <https://doi.org/10.1016/j.apenergy.2017.01.056>
- Haberl JS (1993) Economic calculations for ASHRAE handbook. Texas A&M University. [Report Number:] EST-TR-93-04-07, Energy Systems Laboratory, College Station, Texas
- Deru M, Field K, Studer D, Benne K, Griffith B, Torcellini P, Liu B, Halverson M, Winiarski D, Rosenberg M, Yazdaniyan M, Huang J, Crawley D (2011) U.S. Department of energy commercial reference building models of the national building stock. Report NREL/TP-5500-46861, Golden CO, pp 1–118
- Rooijen JV A life cycle assessment of the PureCell™ stationary fuel cell system: providing a guide for environmental improvement. A report of the Center for Sustainable Systems, Report No. CSS06–09. 30 June 2006 Salt River Project. <http://www.srpnet.com/about/facts.aspx#ownership>. Accessed Aug 2013
- CBCECS Database website. <http://www.eia.gov/consumption/commercial/index.cfm>
- Muller NZ (2014) Toward the measurement of net economic welfare: air pollution damage in the U.S. national accounts–2002, 2005, 2008. In: Jorgenson DW, Landefeld JS, Schreyer P (eds) *Measuring economic sustainability and progress volume*. University of Chicago Press, pp 429–459
- EPA (2015) eGRID 2012 summary tables, 5 Oct 2015
- U.S. Energy Information Agency (EIA) (2011) Voluntary reporting of greenhouse gases program. Emission factors and global warming potentials. http://www.eia.gov/survey/form/eia_1605/emission_factors.html. Accessed Aug 2013, Revised 28 Apr 2011
- U.S. Energy Information Agency (EIA). Total district heat consumption and expenditures. Table C25. Table 1.3–1 and 1.3–4. <http://www.eia.gov/>. Accessed Sep 2013
- Siler-Evans K, Lima Azevedo I, Morgan MG (2012) Marginal emissions factors for the U.S. electricity system. *Environ Sci Technol* 46:4742–4748
- Barbose G, Wiser R, Heeter J, Mai T, Bird L, Bolinger M, Carpenter A, Heath G, Keyser D, Macknick J, Mills A, Millstein D (2016) A retrospective analysis of benefits and impacts of U.S. renewable portfolio standards. *Energy Policy* 96:645–660. ISSN 0301-4215, <https://doi.org/10.1016/j.enpol.2016.06.035>
- Colella WG, Pilli SP (2012) Energy system and thermo-economic analysis of combined heat and power fuel cell systems. In: *Proceedings of the ASME 6th international conference on energy sustainability*, San Diego, 23–25 July 2012. ESFuelCell2012–91481

27. National Energy Technology Laboratory (NETL) (2009) Natural gas-fueled distributed generation solid oxide fuel cell systems. Report Number: R102 04 2009/1
28. White House (2013) Technical support document: technical update of the social cost of carbon for regulatory impact analysis – under executive order 12866 – interagency working group on social cost of carbon, United States Government, May 2013
29. EPA (2015) Regulatory impact analysis for the Clean Power Plan final rule, 23 Oct 2016
30. EPA (2015) Clean Power Plan fact sheet. <http://bio.tech.lsu.edu/blog/fs-cpp-ee.pdf>. Accessed 20 June 2017
31. Siler-Evans K, Azevedo IL, Morgan MG, Apt J (2013) Regional variations in the health, environmental, and climate benefits of wind and solar generation. *Proc Natl Acad Sci* 110:11768–11773
32. Nishizaki K, Hirai K (2009) Commercialization of residential PEM fuel cell CHP “ENE FARM”, White paper by Tokyo Gas Co. and Osaka Gas Co.
33. ACI Technologies, Inc. (2011) Manufacturing fuel cell Manhattan project, Report under U.S. government contract no. N00014–08-D-0758
34. Prugh DN, Tannenbaum HP (2009) U.S. Patent, US 20090169950
35. Heinzl A et al (2004) Injection moulded low cost bipolar plates for PEM fuel cells. *J Power Sources* 131(1):35–40
36. Yeetsom R, Fowler M, Tzoganakis C, Yuhua W, Taylor M (2008) Polypropylene composites for polymer electrolyte membrane fuel cell bipolar plates. *Macromol Symp* 264:34–43
37. Yeetsom R, Fowler M, Tzoganakis C (2011) A review of thermoplastic composites for bipolar plate materials in PEM fuel cells, Chapter 16. In: Cuppoletti J (ed) *Nanocomposites with unique properties and applications in medicine and industry*. InTech, Rijeka
38. Chien JM (2013) Ph.D. dissertation, University of California, Berkeley
39. Incropera FP, DeWitt DP, Bergman TL, Lavine AS (2007) *Fundamentals of heat and mass transfer*. <https://doi.org/10.1016/j.applthermaleng.2011.03.022>
40. Rafferty KD (1998) Heat exchangers, pp 261–277. <http://www.oit.edu/docs/default-source/geoheat-center-documents/publications/heat-exchangers/tp54.pdf?sfvrsn=2>
41. Stevenson J (2003) Paper presented at the SOFC seal meeting, SECA core technology program. Sandia National Laboratory, Albuquerque
42. Jung GB (2013) Can be found under <http://www.enedu.org.tw/files/DownloadFile/20131010130452.pdf>
43. Ghezal Ayagh H (2014) Paper presented at the 15th annual SECA workshop, National energy technology laboratory, Pittsburgh
44. Borglum B (2008) Development of solid oxide fuel cells at Versa Power Systems. In: Williams M, Krist K, Garland N (eds) *ECS transactions, fuel cell seminar 2008*. The electrochemical society, Pennington, pp 9–13
45. Carlson EJ, Yang Y, Fulton C (2004) Tiax report for national energy technology laboratory
46. H.K. Woodward (2003) M.S. Thesis, Worcester Polytechnic Institute, Worcester
47. Schafbauer W, Menzler NH, Buchkremer HP (2014) Tape casting of anode supports for solid oxide fuel cells at Forschungszentrum Jülich. *Intl J App Ceramic Tech* 11:125–135
48. Thorel A (2010) Tape casting ceramics for high temperature fuel cell applications. In: Wunderlich W (ed) *Ceramic materials*. InTech, Rijeka, pp 49–67
49. Liu Q L et al (2011) IOP Conf. Ser.: Mater. Sci. Eng. 18 132006. <https://doi.org/10.1088/1757-899X/18/13/132006>
50. Mistler RE, Runk RB, Shanefield DJ (1978) Tape casting of ceramics. In: Onoda GY, Hench LL (eds) *Ceramic processing before firing*. Wiley, New York, pp 411–448
51. Battelle Memorial Institute (2014) Report for U.S. Department of energy under Contract No. DE-EE0005250
52. Burggraaf AJ, Cot L (1996) *Fundamentals of inorganic membrane science and technology*. Elsevier, Amsterdam
53. Weimar MR, Gotthold DW, Chick LA, Whyatt GA (2013) Cost study for manufacturing of solid oxide fuel cell power systems, PNNL-22732. Pacific Northwest National Laboratory, Richland
54. Breunig HM (2015) Parameter variation and scenario analysis in impact assessments of emerging energy technologies. University of California, Berkeley

Reviews and Other References

- Bar-On I, Kirchain R, Roth R (2002) Technical cost analysis for PEM fuel cells. *J Power Sources* 109:71–75
- Mehta V, Cooper JS (2003) Review and analysis of PEM fuel cell design and manufacturing. *J Power Sources* 114:32–53
- Sopian K, Wan Daud WR (2006) Challenges and future developments in proton exchange membrane fuel cells. *Renew Energy* 31:719–727
- Tietz F, Buchkremer HP, Stöver D (2002) Components manufacturing for solid oxide fuel cells. *Solid State Ionics* 152–153:373–381
- Verrey J, Wakeman MD, Michaud V, Månson J-AE (2006) Manufacturing cost comparison of thermoplastic and thermoset RTM for an automotive floor pan. *Compos A: Appl Sci Manuf* 37:9–22
- Wannek C, Glösen A, Stolten D (2010) Materials, manufacturing technology and costs of fuel cell membranes. *Desalination* 250:1038–1041